arXiv:0907.1264v2 [math-ph] 2 Sep 2009

The arctic curve of the domain-wall six-vertex model

F. Colomo and A.G. Pronko

Abstract. The problem of the form of the 'arctic' curve of the six-vertex model with domain wall boundary conditions in its disordered regime is addressed. It is well-known that in the scaling limit the model exhibits phase-separation, with regions of order and disorder sharply separated by a smooth curve, called the arctic curve. To find this curve, we study a multiple integral representation for the emptiness formation probability, a correlation function devised to detect spatial transition from order to disorder. We conjecture that the arctic curve, for arbitrary choice of the vertex weights, can be characterized by the condition of condensation of almost all roots of the corresponding saddle-point equations at the same, known, value. In explicit calculations we restrict to the disordered regime for which we have been able to compute the scaling limit of certain generating function entering the saddle-point equations. The arctic curve is obtained in parametric form and appears to be a non-algebraic curve in general; it turns into an algebraic one in the so-called root-of-unity cases. The arctic curve is also discussed in application to the limit shape of q-enumerated (with $0 < q \leqslant 4$) large alternating sign matrices. In particular, as $q \to 0$ the limit shape tends to a nontrivial limiting curve, given by a relatively simple equation.

1. Introduction

In strongly correlated systems, the effect of boundary conditions can be relevant even in the thermodynamic limit. Consider for example a system whose parameters are tuned in such a way that at equilibrium it should be in a disordered phase, while its boundary conditions are chosen so that only ordered configurations are admissible in the proximity of the boundary. Due to the presence of strong correlations, it may happen that such boundary conditions induce ordered regions extending macroscopically from the boundaries deeply inside the bulk of the system. In such situation, spatial phase separation emerges, with ordered regions contiguous to the boundary, sharply separated from a central disordered region by a smooth curve, called arctic curve in the case of dimer models [1].

Essentially the same phenomena appear in other contexts, with different names, such as limit shape (in the statistics of Young diagrams [2] and rhombi tilings [3]), or interface (in random growth models for two-dimensional crystals [4]). More generally, the problem consists in finding the limit shapes and fluctuations of random two-dimensional surfaces arising, for instance, in plane partitions (or in three-dimensional Young diagrams, or in the melting of a faceted crystal) [5–7], and also in dimer models on planar bipartite graphs with fixed boundary conditions, when

described in terms of the height function [8, 9]. For recent developments see, e.g., [10, 11]. In these contexts, the arctic curve is usually referred to as the frozen boundary of the limit shape.

The standard example of an arctic curve is the famous arctic circle which appeared in the study of domino tilings of large Aztec diamonds [1, 12]. The name originates from the fact that in most configurations the dominoes are 'frozen' outside the circle inscribed into the diamond, while the interior of the circle is a disordered, or 'temperate', zone. Further investigations of the domino tilings of Aztec diamonds, such as details of statistics near the circle, were also performed [13–15].

In the present paper we address the problem of the form of the arctic curve in the six-vertex model with domain wall boundary conditions. The case of generic Boltzmann weights of the disordered regime is considered. We find an explicit expression for the curve in a parametric form; in general, the curve appears to be non-algebraic. This property can be ascribed to the fact that the six-vertex model cannot be reduced to a model of discrete free (or Gaussian) fermions.

Indeed, in all examples considered to date, the arctic curves appear to be algebraic curves. At the same time, these examples can be seen as particular realizations of models of discrete free fermions, although on various types of lattice and with nontrivial boundary conditions. Some of them can be even reformulated as the six-vertex model at its free-fermion point with suitably chosen fixed boundary conditions (the correspondence being however usually not bijective). In particular, this is the case of domino tilings of Aztec diamonds, and the corresponding boundary conditions of the six-vertex model are exactly the domain wall ones [12, 16]. Thus the problem of the arctic curve extends naturally to the six-vertex model with generic weights, and with fixed (in particular, domain wall) boundary conditions. The phenomenon of phase separation for six-vertex model, in various regimes and with various fixed boundary conditions, was studied previously mainly numerically [17–19]; some analytical approaches to treat the problem were discussed in [20, 21].

Historically, the six-vertex model with domain wall boundary conditions was introduced to prove the Gaudin hypothesis for norms of Bethe states [22]. The standard framework for the model is the quantum inverse scattering method, invented in seminal paper [23]; for a review and applications of the method see book [24]. The partition function of the model was obtained in terms of a determinant, known as Izergin-Korepin formula [25, 26]. The free energy per site was derived in [27, 28], where phase separation was proposed as a possible explanation for the observed influence of boundary conditions on the thermodynamic properties. This, in turn, stimulated subsequent exact calculation of correlation functions of the domain-wall six-vertex model for generic values of its weights. This was done, using the quantum inverse scattering method, for one- and two-point boundary correlation functions [29, 30], and, more recently, also for a particular non-local correlation function, the so-called emptiness formation probability [31].

The interest in the domain-wall six-vertex model is also motivated by its close relationship with some problems in algebraic combinatorics. Apart from the already mentioned domino tilings of Aztec diamond, the model was also found to be related with enumerations of alternating sign matrices [12]. This observation was useful since it opened new possibilities in proving long-standing conjectures in this subject [32, 33]; see also book [34] for a review. In this context the arctic curve of the

domain-wall six-vertex model is of great interest since it describes the limit shape of very large alternating sign matrices [35, 36].

In the present paper, to address the problem of the arctic curve, we develop the idea proposed in [31] of studying the scaling limit of the emptiness formation probability, a correlation function with the capability of detecting spatial transition from order to disorder. Namely, in the scaling limit the emptiness formation probability may have only a simple step-function behaviour, when varying coordinates from ordered to disordered regions, with the jump from one to zero occurring exactly at the arctic curve (actually, at one of its four portions, see Sections 2.3 and 4.1 for details). This can be seen as a particular case of the general statement that the probability of finding a macroscopically large ordered sub-region must vanish in the disordered region. The arctic curve can then be obtained from certain multiple integral representation for the emptiness formation probability, as the condition on the relevant parameters (scaled coordinates) ensuring such a stepwise behaviour in the scaling limit.

This programme was first fulfilled in [37] for a particular choice of the parameter Δ of the six-vertex model, the case $\Delta = 0$, also known as the free-fermion point of the model. In that paper it is observed that the arctic curve can be obtained by investigating the multiple integral representation for emptiness formation probability derived in [31]. It was found that the arctic curve corresponds to a rather peculiar solution of the system of saddle-point equations, namely, the solution characterized by a trivial Green function, with just one pole. In other words, the arctic curve appears to be in correspondence with the condition of 'condensation' of almost all saddle points at the same value in the complex plane. In the case of $\Delta = 0$ this correspondence, between the condensation and the arctic curve, admits a rigorous derivation since in this case the saddle-point equations can be analysed using standard methods from the theory of random matrix models (although some complication arises, due to the two-cut nature of the problem, see Section 5.2, or also [37], for details).

In the case of generic values of Δ, i.e., away from the free-fermion point, the system of coupled saddle-point equations describing the scaling limit of the emptiness formation probability is extremely intricate and the standard tools of random matrix models (e.g., the Green function approach) are inapplicable. We conjecture that the arctic curve can nevertheless be found as the condition of condensation of almost all roots of the saddle-point equations to the same, known, value. As already observed in [36], certain specific properties of the investigated multiple integral representation, guaranteeing the step-function behaviour of the emptiness formation probability in the scaling limit, appear to be totally independent of the values of the parameters of the model, in particular, of the value of Δ. We also propose a method for deriving the arctic curve without a direct use of the Green function, but rather exploiting the fact that in the case of condensation the system of coupled saddle-point equations simplifies to a single equation (that we call 'reduced saddle-point equation'). This equation must necessarily have two coinciding real roots, for consistency with condensation itself. The arctic curve is then given as the condition of coincidence of two roots of the reduced saddle-point equation, where the value of this double root is the parameter which parameterizes the curve.

To obtain the explicit form of the reduced saddle-point equation, and hence to derive the arctic curve, one has also to find the thermodynamic limit of certain function, which plays the role of generating function of a particular one-point boundary correlation function. Here we evaluate this limit for the whole disordered regime, thus extending the results of [36] where two relevant particular cases away from the free-fermion point were considered. We also give here a detailed exposition of the method.

The organization of the present paper mainly follows the logic of our derivation of the main result. After recalling the definition of the model, Izergin-Korepin formula, and the phase separation in Section 2, in Section 3 we introduce boundary correlation functions and address the problem of finding the contact points of the arctic curve with the boundaries, in the disordered regime. The definition of the emptiness formation probability, the multiple integral representation for this correlation function, and the corresponding scaling limit saddle-point equations are given in Section 4. We devote Section 5 to a derivation of the arctic curve at the free-fermion point of the model. Here we also explain how to derive the arctic curve without any use of the Green function but through the simpler condition of coincidence of two roots of the reduced saddle-point equation. In Section 6 we show that the two specific properties of the multiple integral representation for the emptiness formation probability which are relevant for the correspondence between the arctic curve and condensation are totally independent of the value of Δ. Here we also derive the reduced saddle-point equation and obtain the arctic curve in the disordered regime ($|\Delta| < 1$); formulae (6.17)–(6.19) constitute the main result of the present paper.

In Section 7, we discuss some particular cases of the main result, also in connection with application of the model to the problem of q-enumeration of alternating sign matrices (with $0 < q \leqslant 4$). In particular, we show that the limit shape of q-enumerated alternating sign matrices has a non-trivial limit as $q \to 0$; with a suitable choice of coordinates the corresponding limiting curve is just the cosine curve. In Section 8 we summarize the results and provide some concluding remarks.

The text is followed by two appendices. In Appendix A we recall some results on the connection between the Izergin-Korepin formula and the generating function of a particular one-point boundary correlation function. In Appendix B we obtain, for the disordered regime, the thermodynamic limit of this generating function, which is essentially used for the derivation of the main result.

2. Six-vertex model, domain wall boundary conditions, and phase separation

2.1. The model. The six-vertex model is canonically formulated in terms of arrows pointing along the edges of a square lattice. The arrows must obey the 'ice-rule': there are two arrows pointing away from, and two arrows pointing into, each lattice vertex.

Equivalently, one can describe the states of the edges in terms of variables taking two values, e.g., $0, 1$. We shall use the convention that such a variable takes value 0 (1) if the arrow on the edge is pointing upward or right (downward or left). Let us consider a single vertex of the square lattice and let μ, ν, ν' and μ' be the variables attached to the left, bottom, top, and right edges of the vertex respectively. Let $w(\mu, \nu, \nu', \mu')$ denote the Boltzmann weight associated with the

vertex. In the six-vertex model

$$w(\mu,\nu,\nu',\mu') = 0 \quad \text{if} \quad \mu+\nu \neq \mu'+\nu'. \tag{2.1}$$

Imposing the arrow-reversal invariance of the Boltzmann weights, we set

$$\begin{aligned} w(0,0,0,0) &= w(1,1,1,1) = a, \\ w(0,1,1,0) &= w(1,0,0,1) = b, \\ w(0,1,0,1) &= w(1,0,1,0) = c, \end{aligned} \tag{2.2}$$

where a, b, and c are some real positive constants, referred often below as 'weights'.

The partition function of the six-vertex model can be defined as

$$Z = \sum_{\{\mu\},\{\nu\}} \prod_{i,j} w(\mu_{i,j},\nu_{i,j},\nu'_{i,j},\mu'_{i,j}). \tag{2.3}$$

Here the product is taken over vertices of the lattice and the sum is performed over values of edge variables; the variables are subject to the linking conditions

$$\mu'_{i,j} = \mu_{i-1,j}, \qquad \nu'_{i,j} = \nu_{i,j-1}. \tag{2.4}$$

To define completely the model, one has also to specify the boundary conditions in (2.3). We shall consider the so-called domain wall boundary conditions, defined below.

From the analysis of thermodynamic limit of the model with periodic boundary conditions (see, e.g. [38]) it is well known that the model has three physical regimes, or phases; two of them are regimes of order and one is a regime of disorder. Let us introduce the parameter

$$\Delta = \frac{a^2+b^2-c^2}{2ab}\,. \tag{2.5}$$

The case $\Delta > 1$ is called ferroelectric regime. Depending on whether $a > b$ or $a < b$, ground state configurations are built from vertices of weight a, or b; in these configurations all arrows are ordered ferroelectrically. The case $\Delta < -1$ is called anti-ferroelectric regime. In this case, the doubly-degenerated ground state is formed only by vertices of weight c, and thus the directions of arrows alternate along vertical and horizontal rows of the lattice. Finally, the case $|\Delta| < 1$ is called disordered (or critical) regime. In this case typical configurations contain vertices of all three weights; there is no particular order of arrows in these configurations.

All over the paper we use the following parameterization for the weights:

$$a = \sin(\lambda+\eta), \qquad b = \sin(\lambda-\eta), \qquad c = \sin 2\eta. \tag{2.6}$$

We also have

$$\Delta = \cos 2\eta. \tag{2.7}$$

The parameter λ has meaning of a rapidity variable and η is the so-called crossing parameter.

In the case of the disordered regime, i.e., when a, b, and c are such that $|\Delta| < 1$, both λ and η are real and satisfy

$$\eta \leqslant \lambda \leqslant \pi-\eta, \qquad 0 < \eta < \frac{\pi}{2}. \tag{2.8}$$

The other two regimes, the ferroelectric and anti-ferroelectric ones, can be approached by analytic continuation (modulo a purely imaginary common factor for each weight), choosing $\lambda = \mathrm{i}\tilde{\lambda}$, $\lambda = \mathrm{i}\tilde{\eta}$ and $\lambda = \pi/2 + \mathrm{i}\tilde{\lambda}$, $\lambda = \pi/2 + \mathrm{i}\tilde{\eta}$, respectively,

where $\tilde{\lambda}$ and $\tilde{\eta}$ are real, and satisfy some further restrictions to ensure positivity of the weights.

For later reference, let us briefly discuss some symmetries of the model. First, we mention the so-called crossing symmetry. It is a symmetry of the Boltzmann weight under reflection of the vertex with respect to the vertical (horizontal) line, reversing the values of the edge variables on the horizontal (vertical) edges, and exchanging the values $a \leftrightarrow b$. For example, the reflection with respect to the vertical line gives the crossing symmetry relation

$$w(\mu,\nu,\nu',\mu'|\lambda) = w(\bar{\mu}',\nu,\nu',\bar{\mu}|\pi-\lambda). \tag{2.9}$$

Here the bar means that the value of the edge variable must be reversed, i.e., $\bar{\mu}=1$ ($\bar{\mu}=0$) if $\mu=0$ ($\mu=1$). Similarly, one can also consider the reflection with respect to the horizontal line, that gives an analogous relation.

Another useful, and in fact even simpler, property of the six-vertex model Boltzmann weight is its invariance under reflection of the vertex with respect to one or another diagonal,

$$w(\mu,\nu,\nu',\mu'|\lambda) = w(\nu,\mu,\mu',\nu'|\lambda) = w(\nu',\mu',\mu,\nu|\lambda). \tag{2.10}$$

We shall refer to this property as the diagonal-reflection symmetry.

2.2. Domain wall boundary conditions. Consider the six-vertex model on a square lattice obtained by intersection of an equal number of vertical and horizontal lines. Domain wall boundary conditions correspond to fixing the variables on the external edges of the lattice in a specific way, namely, with all arrows on horizontal edges pointing outward the lattice, and all arrows on external vertical edges pointing inward the lattice. Equivalently, these boundary conditions mean that all variables attached to external edges on the top and on the left are set to 1, while those attached to external edges on the bottom and on the right are set to 0.

Denoting by N the number of vertical, or, equivalently, horizontal lines of the lattice on which the model with domain wall boundary conditions is considered, we denote by Z_N the partition function of this model,

$$Z_N = \sum_{\{\mu\},\{\nu\}} \prod_{i,j=1}^{N} w(\mu_{i,j},\nu_{i,j},\nu'_{i,j},\mu'_{i,j})\Big|_{\substack{\mu_{N,*}=\nu'_{*,1}=1\\ \nu_{*,N}=\mu'_{1,*}=0}}. \tag{2.11}$$

Here the stars indicate that the subscripts must run over all possible values, e.g., $\mu_{N,*}=1$ means that $\mu_{N,1}=\mu_{N,2}\cdots=\mu_{N,N}=1$.

In parametrization (2.6), it can be shown that the partition function admits the following exact representation [25]

$$Z_N = \frac{\big[\sin(\lambda-\eta)\sin(\lambda+\eta)\big]^{N^2}}{\prod_{n=1}^{N-1}(n!)^2}\, D_N. \tag{2.12}$$

Here $D_N = D_N(\lambda)$ stands for the Hänkel determinant

$$D_N := \begin{vmatrix} \varphi(\lambda) & \varphi'(\lambda) & \dots & \varphi^{(N-1)}(\lambda) \\ \varphi'(\lambda) & \varphi''(\lambda) & \dots & \varphi^{(N)}(\lambda) \\ \vdots & \vdots & \ddots & \vdots \\ \varphi^{(N-1)}(\lambda) & \varphi^{(N)}(\lambda) & \dots & \varphi^{(2N-2)}(\lambda) \end{vmatrix}, \tag{2.13}$$

where function $\varphi(\lambda)$ is given by

$$\varphi(\lambda) := \frac{\sin 2\eta}{\sin(\lambda-\eta)\sin(\lambda+\eta)}. \tag{2.14}$$

Formula (2.12) follows from the more general result, known as Izergin-Korepin formula (see Appendix A, equation (A.2)), which is valid for the model with inhomogeneous weights [25]. The proof of Izergin-Korepin formula is essentially based on the quantum inverse scattering method [23, 24]; see also [26] for details.

Using formula (2.12) one can study the partition function in the thermodynamic limit. The quantity of interest is the free energy per site f, defined as

$$f := -\lim_{N\to\infty} \frac{\ln Z_N}{N^2}. \tag{2.15}$$

It can be shown [27,28,39] that the free energy per site of the model in the disordered regime is given by the expression

$$f = -\ln\left(\frac{\alpha\sin(\lambda+\eta)\sin(\lambda-\eta)}{\sin\alpha(\lambda-\eta)}\right), \tag{2.16}$$

where we have used the notation

$$\alpha := \frac{\pi}{\pi-2\eta}. \tag{2.17}$$

For a derivation of formula (2.16) see also Appendix B.

Formula (2.16) was obtained for the first time in [27], where also the case of ferroelectric regime was considered; the case of the anti-ferroelectric regime was studied in [28]. In these studies, the following observation have been made: the free energy per site is greater in the case of the domain wall boundary conditions, in comparison with the case of periodic boundary conditions, both for the disordered and anti-ferroelectric regimes, but remains the same for the ferroelectric regime,

$$f_{\text{domain wall}} > f_{\text{periodic}}, \qquad \text{for} \quad \Delta < 1. \tag{2.18}$$

This result can be explained by the fact that in these two regimes, admissible configurations are significantly constrained by the domain wall boundary conditions. Moreover, for large lattices, these effects are macroscopically large, i.e., the model exhibits phase-separation phenomena.

2.3. Phase separation and arctic curves. The six-vertex model exhibits spatial separation of phases for a wide choice of fixed boundary conditions [17]. Roughly speaking, the effect is related to the fact that ordered configurations on the boundary can induce, through the ice-rule, a macroscopic order inside the lattice. Analytically, as already mentioned, a signal for presence of phase separation is a change of the free energy per site, in comparison with the case of periodic boundary conditions.

The notion of phase separation acquires a precise meaning in the scaling limit. This is a thermodynamic limit which is to be treated as a continuum limit, namely, in this limit the number of lines of the lattice (in each direction) tends to infinity and the lattice spacing vanishes, while the total size of the system (in each direction) is kept fixed.

For the domain-wall six-vertex model we take $N \to \infty$, but the whole lattice is scaled to a finite square, e.g., with sides of length 1. Typical configurations are constrained to have macroscopic regions of ferroelectric order near the boundary.

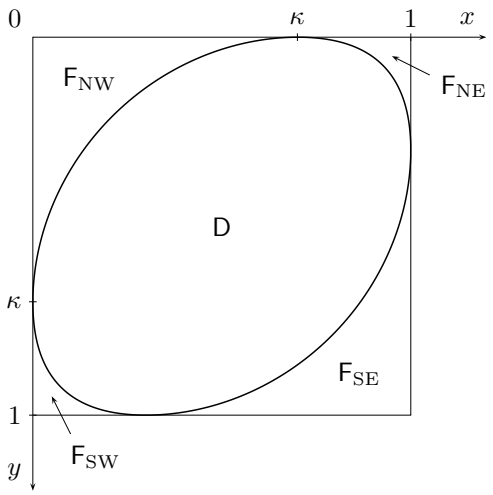


FIGURE 1. The four regions of ferroelectric order and the region of disorder for the model in the scaling limit, in the disordered regime.

More precisely, if the parameters of the model are tuned to the ferroelectric regime then there is full compatibility between boundary and bulk phase, no conflict arises, and the whole system is in the ferroelectric order. If, however, the parameters of the model are tuned to the disordered or the anti-ferroelectric regimes, then there is a competition with the ferroelectric ordering induced by the boundaries, and phase separation emerges. The present understanding of the phase-separation phenomenon in these two regimes is mostly due to numerics [18, 19]; theoretical considerations based on a variational principle approach can be found in [20, 21]. Below we describe the case of disordered regime, and mention briefly the situation in the anti-ferroelectric regime at the end.

In the case of the disordered regime, in the scaling limit five regions appear: four regions of ferroelectric order, $\mathsf{F}_{\rm NW}, \mathsf{F}_{\rm NE}, \mathsf{F}_{\rm SE}, \mathsf{F}_{\rm SW}$ in the four corners of the square, and one region of disorder D, in the centre, see figure 1. The region of disorder is sharply separated by some smooth curve $\mathcal{A}$, called the arctic curve. The arctic curve and the square have four contact points, located each one on a side of the square.

The arctic curve in the disordered regime consists of four portions,

$$\mathcal{A} = \mathit{\Gamma}_{\rm NW} \cup \mathit{\Gamma}_{\rm NE} \cup \mathit{\Gamma}_{\rm SE} \cup \mathit{\Gamma}_{\rm SW}, \tag{2.19}$$

where $\mathit{\Gamma}_i$ separates the region F_i ($i = {\rm NW}, {\rm NE}, {\rm SE}, {\rm SW}$) from the internal region of disorder D.

To describe, for example, the curve $\mathit{\Gamma}_{\rm NW}$, one can introduce a function $\Upsilon(x, y; \lambda)$ where x and y are coordinates in the scaling limit and λ is the parameter of the weights,

$$\mathit{\Gamma}_{\rm NW}: \ \Upsilon(x, y; \lambda) = 0, \qquad x, y \in [0, \kappa]. \tag{2.20}$$

It is to be emphasized, that the explicit form of $\Upsilon(x, y; \lambda)$ is significantly determined by the value of η. Given function $\Upsilon(x, y; \lambda)$ one can readily obtain all other portions

of the arctic curve. Due to the crossing symmetry, relation (2.9), we have

$$\mathit{\Gamma}_{\rm NE}:\ \Upsilon(1-x,y;\pi-\lambda)=0,\qquad x\in[1-\kappa,1],\ y\in[0,\kappa]. \tag{2.21}$$

Exploiting the diagonal-reflection symmetry, we further have

$$\mathit{\Gamma}_{\rm SE}:\ \Upsilon(1-x,1-y;\lambda)=0,\qquad x,y\in[1-\kappa,1]. \tag{2.22}$$

Finally, and essentially similarly, we have

$$\mathit{\Gamma}_{\rm SW}:\ \Upsilon(x,1-y;\pi-\lambda)=0,\qquad x\in[0,\kappa],\ y\in[1-\kappa,1]. \tag{2.23}$$

Thus, knowledge of function $\Upsilon(x,y;\lambda)$ allows one to determine the whole arctic curve $\mathcal{A}$.

It turns out that function $\Upsilon(x,y;\lambda)$ is algebraic (for example, quadratic in x and y) only for special values of η, while in general it is a rather complicated non-algebraic, or transcendental, function. To describe the curve $\mathit{\Gamma}_{\rm NW}$, in practical calculation, we shall use the parametric form

$$x=X(\zeta),\qquad y=Y(\zeta),\qquad \zeta\in[0,\zeta_0], \tag{2.24}$$

where $X(\zeta)$, $Y(\zeta)$ and ζ_0 depend on the parameters of the model, λ and η. This must be taken into account when reconstructing the whole arctic curve $\mathcal{A}$ as explained above. Functions $X(\zeta)$ and $Y(\zeta)$ will be monotonously decreasing and increasing functions, respectively, satisfying $X(0)=\kappa$, $Y(0)=0$ and $X(\zeta_0)=0$, $Y(\zeta_0)=\kappa$. Furthermore, these two functions are in fact just a single function, since, due to reflection symmetry, we have the relation $X(\zeta)=Y(\zeta_0-\zeta)$. The explicit results are given in Section 6, and some interesting particular cases are discussed in Section 7.

To conclude here, we mention briefly that in the case of the anti-ferroelectric regime the picture of phase separation, though reminding the situation of the disordered regime, is more complicated. The competition between the anti-ferroelectric central region and the ferroelectric boundary regions induces the emergence of an intermediate disordered region. As a result, there are two phase-separation curves: an outer one, which is the usual arctic curve, separating the ferroelectric and disordered phases, and an inner one separating the disordered and anti-ferroelectric phases. We refer for further details to [18, 19] where numerical simulations for this regime were performed.

3. Boundary correlation functions

3.1. Definitions and properties. Before addressing the whole problem of the arctic curve, it is useful to restrict first to the simpler problem of the position of the contact points. This problem can be treated by studying correlation functions describing probabilities of certain configurations near the boundaries, the so-called boundary correlation functions.

Following [29], we consider two kinds of boundary correlation functions, denoted as $H_N^{(r)}$ and $G_N^{(r)}$ (in these notations the superscript in parenthesis, r, refers to some distance on the lattice, and should not be confused with an rth derivative with respect to any variable). As it will become clear later, the first correlation function will play a somewhat fundamental role, through its generating function $h_N(z)$ which enters various correlation functions, while the second one is more specific but relevant for addressing the problem of the contact points.

The first correlation function, $H_N^{(r)}$, is designed to reflect the fact that the configurations of the model with domain wall boundary conditions admit one and only one c-weight vertex on each of the four boundary lines of the lattice. Specifically, we define $H_N^{(r)}$ as the probability that the sole c-weight vertex of the first horizontal line from the top occurs at the rth position from the right. It can be introduced by the formula

$$H_N^{(r)} = Z_N^{-1} \sum_{\{\mu\},\{\nu\}} \delta(\mu_{r,1},1)\delta(\mu'_{r,1},0) \prod_{i,j=1}^{N} w(\mu_{i,j},\nu_{i,j},\nu'_{i,j},\mu'_{i,j}) \Big|_{\substack{\mu_{N,*}=\nu'_{*,1}=1 \\ \nu_{*,N}=\mu'_{1,*}=0}}, \quad (3.1)$$

where $\delta(\mu,\mu')$ stands for the Kronecker symbol,

$$\delta(\mu,\mu') := \begin{cases} 1 & \text{if} \quad \mu = \mu' \\ 0 & \text{if} \quad \mu \neq \mu' \end{cases}. \quad (3.2)$$

This correlation function, satisfies the sum-rule

$$\sum_{r=1}^{N} H_N^{(r)} = 1, \quad (3.3)$$

which simply expresses the fact that the total probability of finding a c-weight vertex anywhere in the first horizontal is exactly one.

Some properties of correlation function $H_N^{(r)}$ can be obtained using the symmetries of the model. In particular, crossing symmetry implies

$$H_N^{(r)}(\lambda) = H_N^{(N-r+1)}(\pi - \lambda). \quad (3.4)$$

Using the diagonal-reflection symmetry, one finds that function $H_N^{(r)}$ also gives, for example, the probability that the sole c-weight vertex on the rightmost vertical line occurs at rth position from the top.

The second correlation function, $G_N^{(r)}$, is defined as the probability of finding a given state on a horizontal edge of the first line, i.e., it is a particular case of polarization. For $r = 1,\dots,N-1$ we define this correlation as the probability of having the edge variable fixed to one, on the edge connecting rth and $(r+1)$th vertices (from the right) of the first horizontal line (from the top),

$$G_N^{(r)} = Z_N^{-1} \sum_{\{\mu\},\{\nu\}} \delta(\mu_{r,1},1) \prod_{i,j=1}^{N} w(\mu_{i,j},\nu_{i,j},\nu'_{i,j},\mu'_{i,j}) \Big|_{\substack{\mu_{N,*}=\nu'_{*,1}=1 \\ \nu_{*,N}=\mu'_{1,*}=0}}. \quad (3.5)$$

We can also set $G_N^{(N)} = 1$ and $G_N^{(0)} = 0$ since the edge variables on the leftmost and the rightmost external edges are already fixed by the boundary conditions to $\mu_{N,1} = 1$ and $\mu'_{1,1} = 0$.

As noticed in [29], correlation functions $H_N^{(r)}$ and $G_N^{(r)}$ are in fact closely related. Indeed, since $\delta(\mu_{r,1},1) + \delta(\mu_{r,1},0) = 1$, formulae (3.1) and (3.5) imply that $G_N^{(r)} = H_N^{(r)} + G_N^{(r-1)}$. Taking into account that $G_N^{(0)} = 0$, one can equivalently bring this relation into the form

$$G_N^{(r)} = H_N^{(r)} + H_N^{(r-1)} + \cdots + H_N^{(1)}. \quad (3.6)$$

Recalling relation (3.3), we obtain that (3.6) implies that $G_N^{(N)} = 1$, in agreement with the definition of this correlation function.

As we shall see below, in the scaling limit function $G_N^{(r)}$ turns into a step function; the point where its value jumps from 0 to 1 is exactly the contact point of the arctic curve. Relation (3.6) and certain properties of function $H_N^{(r)}$ will allow us to find the location of this point.

3.2. Function $h_N(z)$ and its large N limit. The correlation function $H_N^{(r)}$ can be equivalently considered through its generating function

$$h_N(z) := \sum_{r=1}^{N} H_N^{(r)} z^{r-1}. \tag{3.7}$$

Due to (3.3), the generating function satisfies the normalization condition $h_N(1) = 1$. For later referring, let us also mention the property

$$h_N(0) = H_N^{(1)} = \frac{c a^{2N-2} Z_{N-1}}{Z_N}. \tag{3.8}$$

This property simply follows from the fact that the c-weight vertex appearing in the corner induces domain wall boundary conditions on the remaining $(N-1)$-by-$(N-1)$ sub-lattice [40]. We have also the relation

$$h_N(z;\lambda) = z^{N-1} h_N(z^{-1};\pi-\lambda), \tag{3.9}$$

which is a direct consequence of relation (3.4).

Given function $h_N(z)$, and taking into account relation (3.6), one can readily represent correlation function $G_N^{(r)}$ as follows

$$G_N^{(r)} = -\frac{1}{2\pi \mathrm{i}} \oint_{C_0} \frac{h_N(z)}{(z-1)z^r}\,\mathrm{d}z. \tag{3.10}$$

Here C_0 is a simple closed counterclockwise-oriented contour surrounding point $z = 0$, and lying in its small vicinity. In the next Section, a much less trivial example of correlation function will be given, where a multi-variable generalization of function $h_N(z)$ will appear.

In [29], where the boundary correlation functions were introduced, it was shown that they can be expressed similarly to formula (2.12) for the partition function, but with properly modified entries in the last column of the determinant. Here we rely on a similar but actually different representation, which relates generating function $h_N(z)$ with the partition function of the 'partially' inhomogeneous model with a single parameter of inhomogeneity. This representation is discussed in detail in Appendix A, see equations (A.8) and (A.12).

The following result plays a crucial role for what follows.

In the disordered regime, i.e., with λ and η satisfying (2.8), the function $\ln h_N(z)$, for z real and non-negative, has the following $N \to \infty$ behaviour

$$\ln h_N(\gamma(\xi)) = N \ln\left(\frac{\sin\alpha(\lambda-\eta)\sin(\xi+\lambda-\eta)\sin\alpha\xi}{\alpha\sin(\lambda-\eta)\sin\alpha(\xi+\lambda-\eta)\sin\xi}\right) + o(N), \tag{3.11}$$

where

$$\gamma(\xi) = \frac{\sin(\lambda+\eta)\sin(\xi+\lambda-\eta)}{\sin(\lambda-\eta)\sin(\xi+\lambda+\eta)} \tag{3.12}$$

and α has been defined in (2.17).

The proof of (3.11) is given in Appendix B.

3.3. Contact points. To find the contact points in the disordered regime, i.e., the value of constant κ, we study correlation function $G_N^{(r)}$ in the scaling limit. Let us define function $G(x)$ $(0 \leqslant G(x) \leqslant 1)$ as the scaling limit of correlation function $G_N^{(r)}$,

$$G(x) := \lim_{r,N\to\infty} G_N^{(r)}, \qquad x = \frac{N-r}{N}, \qquad x \in [0,1]. \tag{3.13}$$

In the scaling limit, the dominating configurations are such that all edge variables for horizontal edges of the first line are fixed to 1 in the region F_{NW}, and to 0 in the region F_{NE}. Therefore, $G(x)$ must have a simple stepwise behaviour, with the jump occurring precisely at the contact point,

$$G(x) = \begin{cases} 1 & \text{for} \quad 0 \leqslant x < \kappa \\ 0 & \text{for} \quad \kappa < x \leqslant 1 \end{cases}. \tag{3.14}$$

Hence, the value of κ can be found by addressing the question of how correlation function $G_N^{(r)}$ may exhibit a stepwise behaviour, as $N, r \to \infty$.

To address this question, we consider integral representation (3.10), and apply the saddle-point technique to analyze its behaviour in the scaling limit. Formally, the saddle-point equation reads

$$-\frac{1-x}{z} + \left(\lim_{N\to\infty} \frac{\ln h_N(z)}{N}\right)' = 0. \tag{3.15}$$

In principle, to investigate the solution of the saddle-point equation, one would need to know the last term in (3.15) for z everywhere in the complex plane. However, it turns out that in addressing the problem of contact points the complete saddle-point analysis can be avoided, once the mechanism at the origin of the stepwise behaviour of function $G(x)$ is understood. Furthermore, formula (3.11), which was derived under the assumption of z being real and positive, appears to be sufficient.

Indeed, let us first restrict to the case $\Delta = 0$, where function $h_N(z)$ is given by a simple explicit expression, $h_N(z) = [\frac{1}{2}(1-\sin 2\lambda)z + \frac{1}{2}(1+\sin 2\lambda)]^{N-1}$, see [29, 41] for a proof. From this expression it follows that the saddle-point equation has only one solution, which we denote by $z_{\mathrm{s.p.}}$. It can be seen that $z_{\mathrm{s.p.}}$, which depends on the value of $x \in [0,1]$, is always real and positive, with the corresponding steepest-descent contour perpendicular to the real axis. When deforming the contour C_0 in (3.10) to the steepest-descent contour, the position of the saddle-point $z_{\mathrm{s.p.}}$ with respect to the pole at $z = 1$ of the integrand appears to be crucial. Namely, for $z_{\mathrm{s.p.}} < 1$, the pole at $z = 1$ can simply be ignored in the deformation of the contour, and the saddle-point evaluation of the integral vanishes in the scaling limit. On the other hand, for $z_{\mathrm{s.p.}} > 1$, in deforming the contour through the saddle-point, we necessarily cross the pole at $z = 1$, thus picking a contribution equal to minus the residue of the integrand at this pole. This mechanism is at the origin of the stepwise behaviour of $G(x)$, with the step occurring when x is such that $z_{\mathrm{s.p.}} = 1$. This last condition thus determines the position of the contact point.

When considering the problem for generic values of Δ, we note that $h_N(z)$, being a polynomial, is analytic, and the only pole to be taken into account in the integrand of (3.10) is again the one at $z = 1$, with residue -1, due to the property $h_N(1) = 1$. Moreover, it can be verified that saddle-point equation (3.15) has only one solution when z is real and positive, as assumed in formula (3.11). The stepwise behaviour of $G(x)$ can thus be ascribed again to the fact that, for some particular

value $x = \kappa \in [0, 1]$, this real and positive saddle-point occurs at $z = 1$. This immediately determines the value of the contact point,

$$\kappa = 1 - \left(\lim_{N\to\infty} \frac{\ln h_N(z)}{N} \right)' \Big|_{z=1}. \tag{3.16}$$

It is apparent that, for the evaluation of the contact point, the knowledge of the large N behaviour of $\ln h_N(z)$ for z real and positive, formula (3.11), is sufficient.

From expression (3.16), and asymptotic behaviour (3.11), in the case of generic value of Δ in the disorder regime, we obtain the following explicit expression

$$\kappa = \frac{\alpha \cot \alpha(\lambda - \eta) - \cot(\lambda + \eta)}{\cot(\lambda - \eta) - \cot(\lambda + \eta)}. \tag{3.17}$$

Note that, under the replacement $\lambda \mapsto \pi - \lambda$, we have $\kappa \mapsto 1 - \kappa$, as expected, due to the crossing symmetry. In particular, for $\lambda = \pi/2$ we have $\kappa = 1/2$ for all values of η in the disordered regime.

4. Emptiness formation probability

4.1. Definition and basic properties. We want now to address the problem of finding the arctic curve $\mathcal{A}$ for the domain-wall six-vertex model. The most direct way would be to consider a one-point correlation function, such as polarization of all horizontal (or vertical) edges on the lattice, compute for it a suitable representation, and finally investigate its behaviour in the scaling limit. This would give access not only to the arctic curve $\mathcal{A}$ but to the whole 'limit shape' of the model, in its 'height function' formulation, in the sense of [21]. The main obstruction for such strategy resides in the difficulty of computing explicitly such one-point correlation function. If one restricts to the arctic curve, however, it is possible to devise some other correlation function, maybe rougher than polarization, but nevertheless refined enough to discriminate the spatial transition between order and disorder, and simpler to calculate.

Indeed, consider the emptiness formation probability (EFP), namely, the probability $F_N^{(r,s)}$ of having the edge variables fixed to 1 on the first s horizontal edges, from the top of the lattice, and located between the rth and $(r+1)$th vertical lines, from the right [31]

$$F_N^{(r,s)} = Z_N^{-1} \sum_{\{\mu\},\{\nu\}} \delta(\mu_{r,1}, 1)\delta(\mu_{r,2}, 1) \cdots \delta(\mu_{r,s}, 1) \times \prod_{i,j=1}^{N} w(\mu_{i,j}, \nu_{i,j}, \nu'_{i,j}, \mu'_{i,j}) \Big|_{\substack{\mu_{N,*}=\nu'_{*,1}=1 \\ \nu_{*,N}=\mu'_{1,*}=0}}. \tag{4.1}$$

Evidently, EFP is just a particular case of a general s-point correlation function, but it enjoys specific properties, outlined below, which are suitable to address the problem of the arctic curve of the model in the disordered regime.

By construction, EFP as defined in (4.1) actually measures the probability that the edge variables of all edges in the top-left $(N - r) \times s$ sub-lattice are fixed to 1. This follows directly from the definition of the six-vertex model, see condition (2.1), and the domain wall boundary conditions. In other words, EFP measures the probability that the top-left $(N - r) \times s$ sub-lattice has ferroelectric order,

To find the arctic curve, one must address the asymptotic behaviour of EFP in the scaling limit. Namely, we are interested in the limit $N, r, s \to \infty$, while keeping the ratios fixed. We set

$$x := \frac{N-r}{N}, \qquad y := \frac{s}{N}, \qquad x, y \in [0,1]\,. \tag{4.2}$$

In this limit, coordinates x and y will parameterize the unit square to which the lattice is rescaled. Correspondingly, EFP is expected to approach some limiting function

$$F(x,y) := \lim_{N,r,s\to\infty} F_N^{(r,s)}. \tag{4.3}$$

Since EFP measures the probability that the top-left $(N-r)\times s$ sub-lattice has ferroelectric order, in the scaling limit, $F(x,y)$ should tend to 1 whenever $(x,y) \in \mathsf{F}_{\mathrm{NW}}$. On the other hand, in the disorder region, by definition, the number of edges breaking the ferroelectric order is macroscopic. Thus, as soon as (x,y) enters the disordered region D, function $F(x,y)$ should immediately vanish. As a result, in the disordered regime, the limiting function is just the step function,

$$F(x,y) = \begin{cases} 1 & \text{if} \quad x,y \in \mathsf{F}_{\mathrm{NW}} \\ 0 & \text{if} \quad x,y \in \mathsf{D} \cup \mathsf{F}_{\mathrm{NE}} \cup \mathsf{F}_{\mathrm{SE}} \cup \mathsf{F}_{\mathrm{SW}} \end{cases}, \tag{4.4}$$

where we have used notations of figure 1.

Hence, EFP can be used to find curve Γ_{NW}, which separates region F_{NW} from the remaining part of the unit square. We recall, see Section 2.3, that knowledge of curve Γ_{NW} allows one to recover other portions Γ_{NE}, Γ_{SE}, and Γ_{SW}, thus solving the problem of the arctic curve of the model.

Curve Γ_{NW} can be found by analysing a suitable representation for EFP in the scaling limit. Moreover, formula (4.4) implies that in such an analysis, similarly to the case of the contact point considered in Section 3.3, understanding the mechanism at the origin of the stepwise behaviour of EFP in the limit is sufficient for finding the curve.

4.2. Multiple integral representations. In the following we resort to the representation for the emptiness formulation probability in terms of s-fold integral obtained in [31]. The calculation itself is based on the quantum inverse scattering method [23, 24] and it represents further development of ideas of [29, 42] where boundary correlation functions were studied. In fact, for what follows we need two equivalent multiple integral representations, which differ only in their integrand, one being just the totally symmetrized version of the other.

To give these representations we need to introduce some notations first. For $s = 1, \ldots, N$, let us define functions $h_{N,s}(z_1, \ldots, z_s)$, where the second subscript refers to the number of arguments, by the formula

$$\begin{aligned} h_{N,s}(z_1,\ldots,z_s) := & \prod_{1\leqslant i<k\leqslant s} \frac{1}{z_k - z_i} \\ & \times \begin{vmatrix} z_1^{s-1} h_{N-s+1}(z_1) & \ldots & z_s^{s-1} h_{N-s+1}(z_s) \\ z_1^{s-2}(z_1-1) h_{N-s+2}(z_1) & \ldots & z_s^{s-2}(z_s-1) h_{N-s+2}(z_s) \\ \vdots & \ddots & \vdots \\ (z_1-1)^{s-1} h_N(z_1) & \ldots & (z_s-1)^{s-1} h_N(z_s) \end{vmatrix}. \end{aligned} \tag{4.5}$$

Note that we also have $h_{N,1}(z) = h_N(z)$. The functions $h_{N,s}(z_1, \dots, z_s)$ are symmetric polynomials of degree $(N-1)$ in each variable $z_1, \dots, z_s$. In fact, these functions can be recursively constructed starting with function $h_{N,N}(z_1, \dots, z_N)$, since, due to the structure of (4.5), it is easy to observe the relation

$$h_{N,s}(z_1, \dots, z_{s-1}, 1) = h_{N,s-1}(z_1, \dots, z_{s-1}). \tag{4.6}$$

One more relation of the same kind is

$$h_{N,s}(z_1, \dots, z_{s-1}, 0) = h_N(0) h_{N-1,s-1}(z_1, \dots, z_{s-1}). \tag{4.7}$$

where the value of $h_N(0)$ is given by formula (3.8). As shown in [31, 43], functions $h_{N,s}(z_1, \dots, z_s)$ are closely related to the partition function of the partially inhomogeneous six-vertex model with domain wall boundary conditions, with s nonzero inhomogeneities. This relationship is sketched in Appendix A.

We are now ready to turn to the multiple integral representations. The first multiple integral representation reads:

$$F_N^{(r,s)} = \frac{(-1)^s}{(2\pi \mathrm{i})^s} \oint_{C_0} \cdots \oint_{C_0} \prod_{j=1}^{s} \frac{[(t^2 - 2\Delta t) z_j + 1]^{s-j}}{z_j^r (z_j - 1)^{s-j+1}} \times \prod_{1 \leqslant j < k \leqslant s} \frac{z_j - z_k}{t^2 z_j z_k - 2\Delta t z_j + 1} \, h_{N,s}(z_1, \dots, z_s) \, \mathrm{d}z_1 \cdots \mathrm{d}z_s. \tag{4.8}$$

Here C_0, as before, denotes a simple anticlockwise oriented contour surrounding the point $z = 0$ and no other singularity of the integrand. We use, besides the anisotropy parameter Δ, the asymmetry parameter

$$t := \frac{b}{a}. \tag{4.9}$$

The second, essentially equivalent, representation reads:

$$F_N^{(r,s)} = \frac{(-1)^{s(s+1)/2} Z_s}{s! (2\pi \mathrm{i})^s a^{s(s-1)} c^s} \oint_{C_0} \cdots \oint_{C_0} \prod_{j=1}^{s} \frac{[(t^2 - 2\Delta t) z_j + 1]^{s-1}}{z_j^r (z_j - 1)^s} \times \prod_{\substack{j,k=1 \\ j \neq k}}^{s} \frac{1}{t^2 z_j z_k - 2\Delta t z_j + 1} \prod_{1 \leqslant j < k \leqslant s} (z_k - z_j)^2 \times h_{N,s}(z_1, \dots, z_s) h_{s,s}(u_1, \dots, u_s) \, \mathrm{d}z_1 \cdots \mathrm{d}z_s. \tag{4.10}$$

Here Z_s denotes the partition function of the six-vertex model with domain wall boundary conditions on an $s \times s$ lattice, and

$$u_j := -\frac{z_j - 1}{(t^2 - 2\Delta t) z_j + 1}. \tag{4.11}$$

The integrand of (4.10) is just the symmetrized version of the integrand of (4.8), with respect to permutations of the integration variables $z_1, \dots, z_s$. This follows through certain symmetrization procedure, see Appendix D of [44], and an additional identity proven in [31].

Representations (4.8) and (4.10) hold for all the three regimes of the model.

4.3. Saddle-point equations. We are interested in the behaviour of EFP in the so-called scaling limit, that is in the limit where r, s and N are all large, with the ratios r/N and s/N kept finite (and smaller than 1). In this limit, in principle, EFP can be analysed through the saddle-point method applied to multiple integral representation (4.10).

To find the corresponding system of saddle-point equations, we apply standard arguments (familiar, for example, from the matrix model context) to the integrand of (4.10). We have to use the fact that quantities like $\ln h_{N,s}(z_1,\dots,z_s)$ are of order s^2, and that their derivatives with respect to z_j's are of order s. As a result, we arrive at the following system of coupled saddle-point equations

$$-\frac{s}{z_j-1}-\frac{r}{z_j}+\frac{s(t^2-2\Delta t)}{(t^2-2\Delta t)z_j+1}-\sum_{\substack{k=1\\k\neq j}}^{s}\left(\frac{t^2z_k-2\Delta t}{t^2z_jz_k-2\Delta t z_j+1}\right.$$
$$\left.+\frac{t^2z_k}{t^2z_jz_k-2\Delta t z_k+1}+\frac{2}{z_k-z_j}\right)+\frac{\partial \ln h_{N,s}(z_1,\dots,z_s)}{\partial z_j}$$
$$-\frac{t^2-2\Delta t+1}{[(t^2-2\Delta t)z_j+1]^2}\,\frac{\partial \ln h_{s,s}(u_1,\dots,u_s)}{\partial u_j}=0, \quad (4.12)$$

where $j=1,\dots,s$. In writing this expression we neglect all sub-leading contributions (i.e., estimated as $o(s)$).

As we shall see, although the saddle-point analysis of the multiple integral representation for EFP cannot be actually performed in the full rigour in general, nevertheless we will be able to find the condition on the ratios r/N and s/N which corresponds to the jump from 0 to 1 of EFP in the scaling limit, i.e., to derive the equation for the arctic curve. In many respects, the whole procedure will remind the saddle-point analysis of the single integral (3.10) which allowed us to find the location of the contact point.

5. An example: the case $\Delta = 0$

5.1. Preliminaries. Before to proceed with the general case, it is useful to consider technically the simplest case $\Delta = 0$. The approach described in this section was given in detail in [37]. Our aim here is to recall the main steps of the approach and formulate a modified version of it, which appears sufficiently simple and powerful to be applied to the much more complicated case of generic values of Δ in the disordered regime, $|\Delta|<1$.

In the case $\Delta=0$, or, equivalently, $\eta=\pi/4$, function $h_N(z)$ is known explicitly. It has a very simple form (see, e.g., [41])

$$h_N(z)=\left(\frac{t^2z+1}{t^2+1}\right)^{N-1}, \qquad t=\tan\left(\lambda-\tfrac{\pi}{4}\right). \quad (5.1)$$

The determinant entering the definition of functions $h_{N,s}(z_1,\dots,z_s)$ turns out to reduce simply to a Vandermonde determinant; straightforward calculation gives us

$$h_{N,s}(z_1,\dots,z_s)=\prod_{j=1}^{s}\left(\frac{t^2z_j+1}{t^2+1}\right)^{N-s}\prod_{1\leqslant j<k\leqslant s}\frac{t^2z_jz_k+1}{t^2+1}. \quad (5.2)$$

From this formula, using $u_j = (1-z_j)/(t^2 z_j + 1)$, we also have

$$h_{s,s}(u_1,\dots,u_s) = \prod_{j=1}^{s} \frac{1}{(t^2 z_j+1)^{s-1}} \prod_{1\leqslant j<k\leqslant s} (t^2 z_j z_k + 1). \tag{5.3}$$

Taking into account that in the considered case $Z_s = 1$ (see, e.g., [29]) and hence $Z_s/a^{s(s-1)}c^s = (t^2+1)^{s(s-1)/2}$, we obtain, as a result, that representation (4.10) at $\Delta = 0$ reads:

$$F_N^{(r,s)} = \frac{(-1)^{s(s+1)/2}}{s!(2\pi\mathrm{i})^s (t^2+1)^{s(N-s)}} \oint_{C_0} \cdots \oint_{C_0} \prod_{j=1}^{s} \frac{(t^2 z_j+1)^{N-s}}{z_j^r (z_j-1)^s} \times \prod_{1\leqslant j<k\leqslant s} (z_j - z_k)^2 \,\mathrm{d}z_1 \cdots \mathrm{d}z_s. \tag{5.4}$$

Due to the last factor of the integrand, which is the squared Vandermonde determinant, formula (5.4) naturally recalls the random matrix model partition function, that will be exploited in what follows.

Here we would like also to mention that the last expression can be brought into the form

$$F_N^{(r,s)} = \det Q \tag{5.5}$$

where matrix Q is an s-by-s matrix with the entries

$$Q_{jk} = -\frac{1}{2\pi\mathrm{i}(t^2+1)^{N-s}} \oint_{C_0} \frac{(t^2 z+1)^{N-s}}{z^r (z-1)^s} (z-\theta)^{j-k+s-1} \,\mathrm{d}z. \tag{5.6}$$

Here θ is an arbitrary parameter whose value does not affect the determinant in (5.5). Note that matrix Q has the structure of a Toeplitz matrix, i.e., its entries depend on the indices only through their difference.

The determinant formula (5.5) has the following important implication. Let us consider the quantity

$$I_N^{(r,s)} := \frac{(-1)^{s(s+1)/2}}{s!(2\pi\mathrm{i})^s (t^2+1)^{s(N-s)}} \oint_{C_1^-} \cdots \oint_{C_1^-} \prod_{j=1}^{s} \frac{(t^2 z_j+1)^{N-s}}{z_j^r (z_j-1)^s} \times \prod_{1\leqslant j<k\leqslant s} (z_j - z_k)^2 \,\mathrm{d}z_1 \cdots \mathrm{d}z_s. \tag{5.7}$$

This quantity differs from (5.4) only in the integration contours: here C_1^- is a closed clockwise oriented contour (the minus sign in the superscript indicates negative direction) in the complex plane enclosing point $z = 1$, and no other singularity of the integrand. Since the integrand is kept intact, we have

$$I_N^{(r,s)} = \det S, \tag{5.8}$$

where entries of matrix S differ from those of matrix Q only in the integration contour,

$$S_{jk} = -\frac{1}{2\pi\mathrm{i}(t^2+1)^{N-s}} \oint_{C_1^-} \frac{(t^2 z+1)^{N-s}}{z^r (z-1)^s} (z-\theta)^{j-k+s-1} \,\mathrm{d}z. \tag{5.9}$$

Here θ is again an arbitrary parameter, whose value does not affect the determinant in (5.8). Setting $\theta = 1$, matrix S reduces to an upper-triangular matrix, with all

its diagonal entries equal to 1. Hence

$$I_N^{(r,s)} = 1, \tag{5.10}$$

for all $r, s = 1, \dots, N$. Identity (5.10), together with some other properties of representation (5.4), turns out to be one of the main ingredients entering the derivation of the arctic curve.

5.2. Matrix model approach. We want now to address the asymptotic behaviour in the scaling limit, as defined in Section 4.1, of multiple integral representation (5.4) for EFP in the case $\Delta = 0$. Inspired by the obvious analogy with the large s limit of the partition function of an $s \times s$ Random Matrix Models, we rewrite multiple integral representation (5.4) as follows:

$$F_N^{(r,s)} = \frac{(-1)^{s(s+1)/2}}{s!(1+t^2)^{(1/y-1)s^2}(2\pi i)^s} \oint_{C_0} \cdots \oint_{C_0} \exp\left\{ -s \sum_{j=1}^{s} V(z_j) \right\} \times \prod_{1 \leqslant j < k \leqslant s} (z_j - z_k)^2 \mathrm{d}z_1 \cdots \mathrm{d}z_s \tag{5.11}$$

where the potential is given by

$$V(z_j) = \ln(z_j - 1) + \frac{1-x}{y} \ln z_j - \left(\frac{1}{y} - 1 \right) \ln(t^2 z_j + 1). \tag{5.12}$$

Here we have used the scaling variables x and y introduced in (4.2). The corresponding system of coupled saddle-point equations reads

$$-\frac{1}{z_j - 1} - \frac{1-x}{y z_j} + \frac{(1-y)t^2}{y(t^2 z_j + 1)} + \frac{2}{s} \sum_{\substack{k=1 \\ k \neq j}}^{s} \frac{1}{z_j - z_k} = 0, \tag{5.13}$$

where $j = 1, \dots, s$.

The standard physical picture reinterprets the saddle-point equations as the equilibrium conditions for the position of s particles, each with charge $1/s$, with logarithmic electrostatic repulsion, in an external potential. In the present case the latter is built from three logarithms, and can be seen as generated by three external charges, 1, $(1-x)/y$, and $-(1/y-1)$ at positions 1, 0, and $-1/t^2$, respectively. It is natural to refer to this model as the triple Penner model. Although the simple Penner [45] matrix model has been widely investigated, not so much is known about the more complicate multiple or generalized Penner models. The main ideas we shall use in the following are based on the phenomenon of eigenvalues condensation, typical of Penner models, and nicely described in [46, 47].

To investigate the structure of solutions of the saddle-point equations (5.13) for large s, one can start with introducing the Green function

$$\mathcal{G}(z) := \frac{1}{s} \sum_{j=1}^{s} \frac{1}{z - z_j}, \tag{5.14}$$

which, if the z_j's solves (5.13), has to satisfy some particular differential equation, which can be derived by standard means. In the scaling limit, such differential equation reduces to an algebraic one for the limiting Green function. In principle, the latter can be solved, and an expression for $\mathcal{G}(z)$ can be obtained in the large s limit. In this limit, the poles of $\mathcal{G}(z)$, organize into cuts in the complex plane, and the discontinuities across such cuts define, when real and positive, the density

of solutions of the saddle-point equation as $s \to \infty$. In the present case, however, the Green function $\mathcal{G}(z)$ is not completely determined by the above procedure, since it contains an extra parameter, which can be fixed only implicitly. This is a direct consequence of the 'two-cut' nature of the problem (see [37] for details). The problem of explicitly finding the density of solutions of saddle-point equation (5.13) as $s \to \infty$, for generic values of x, y, is therefore a formidable one, not to mention the evaluation of the corresponding 'free energy', and of the saddle-point contribution to the integral in (5.11).

The problem we are addressing is fortunately much more modest: we are presently interested only in the expression of curve $\mathit{\Gamma}_{\rm NW}$, which, as explained in Section 4.1, corresponds to the curve in the unit square, where, in the scaling limit, EFP has a unit jump. As discussed in Section 3.3, concerning the scaling limit of the boundary correlation function $G_N^{(r)} = F_N^{(r,1)}$, its stepwise behaviour was related to the position of the saddle-point solution with respect to the pole at $z = 1$. It is easy to verify that the same mechanism holds for $F_N^{(r,s)}$ for any finite value of s: indeed, in the $r, N \to \infty$ limit, with s and $r/N = 1 - x$ kept fixed (and, obviously, $s/N = y \to 0$), saddle-point equations (5.13) decouple into s identical saddle-point equations of the form (3.15). The line of reasoning discussed in Section 3.3 can be applied again, and due also to identity (5.10), it is clear that the unit jump defining the position of the contact point occurs now when all s saddle-point solutions are located at $z = 1$.

Before going on to the large s situation, it is worth to recall a peculiar property of the saddle-point solutions for generic Penner models (see [46] and [47] for further details). In these models the logarithmic wells in the potential can behave as condensation germs for the saddle-point solutions. It can be shown that condensation can occur only for charges less than or equal to 1, the value of the charge corresponding to the fraction of condensed solutions. Within the electrostatic analogy, this corresponds to the capability for the logarithmic potential well created by external charge Q to screen exactly a fraction Q of the s particles of charge $1/s$.

In our case, the only possibility for condensation of solutions of the saddle-point equations is given by the charge at $z = 1$ in the triple Penner potential, since the charge at $z = -1/t^2$ is always repulsive, while the one at $z = 0$ is larger than 1 in the region where $\mathit{\Gamma}_{\rm NW}$ lies. Note further that in our case the charge at $z = 1$ is exactly 1, allowing for total condensation of solutions of the saddle-point equations. This consideration, and the crucial identity (5.10), strongly suggests that the mechanism producing the stepwise behaviour of $F_N^{(r,s)}$ in the scaling limit is still the same as in the case of finite s, and thus that the curve $\mathit{\Gamma}_{\rm NW}$ occurs in correspondence to the condensation of (almost) all solutions of saddle-point equations (5.13) at the point $z = 1$

In the framework of the Green function approach, our claim can be rephrased as follows: the curve $\mathit{\Gamma}_{\rm NW}$ can be derived from the condition that x and y should be such that in the scaling limit Green function (5.14) reduces to

$$\mathcal{G}(z) = \frac{1}{z-1}. \tag{5.15}$$

Indeed, in [37] it is shown that this requirement translates into the following condition:

$$(1+t^2)(x+y-1)^2 + t^2(1+t^2)(x-y)^2 = t^2, \tag{5.16}$$

for $x, y \in [0, \kappa]$. Recalling how the remaining portions of the arctic curve can be reconstructed (see discussion in Section 2.3), we also find that equation (5.16) describes the whole curve $\mathcal{A}$, i.e., it is valid for all $x, y \in [0, 1]$. At $\lambda = \pi/2$, or $t = 1$, it turns into $(x - 1/2)^2 + (y - 1/2)^2 = 1/4$, which is the arctic circle of [1].

5.3. Condensation of roots and arctic curve. As just discussed, the arctic curve $\mathit{\Gamma}_{\mathrm{NW}}$ occurs in correspondence to the situation where almost all roots of saddle-point equations (5.13) condense at point $z = 1$. It turns out that this observation can be used to formulate a simpler approach, which does not involve the Green function, and can be extended to more general situations (beyond the case $\Delta = 0$).

The origin of the observed correspondence between the arctic curve $\mathit{\Gamma}_{\mathrm{NW}}$ and the condensation of almost all roots of saddle-point equations relies on the two following important ingredients. On one hand, by construction, EFP in the scaling limit has a stepwise behaviour, the unit jump occurring in correspondence to $\mathit{\Gamma}_{\mathrm{NW}}$. On the other hand, generalized Penner models (whose saddle-point equations share some essential features with the ones under consideration) allow for partial or total condensation of roots. The role of the unit charge potential in a generalized Penner model with total condensation is played in our case by the s poles at $z = 1$ in representation (5.4), which all turn out to be poles of order s.

Having in mind these essential features, the correspondence between the arctic curve and the condensation of roots can be seen as the consequence of the following properties of multiple integral representation for EFP:

- in each integration variable $z_1, \dots, z_s$ the integrand has a pole at $z = 1$, and the cumulative residue over all these variables at this pole is equal to 1;
- the pole at $z = 1$ for each integration variable $z_1, \dots, z_s$ is of order s.

The first property means that the scaling limit of EFP is governed by the position of the roots of saddle-point equations with respect to the pole at $z = 1$, and, furthermore, identity (5.10) implies that deforming the integration contours trough this pole produces exactly the expected stepwise limiting expression for EFP. The second property means that point $z = 1$ is the point where the condensation of almost all roots of the corresponding saddle-point equations may occur.

The properties listed above, together with the expected limiting expression (4.4), implies that the arctic curve can be found through the condition of condensation of almost all roots of the saddle-point equations at $z = 1$. Let n_c and n_u denote the number of condensed and uncondensed roots, respectively, $n_c + n_u = s$. Condensation of 'almost all' roots, simply means that

$$\frac{n_c}{s} \sim 1, \qquad \frac{n_u}{s} \sim 0, \qquad s \to \infty. \tag{5.17}$$

Note that condensation of almost all roots at $z = 1$ evidently implies formula (5.15) and also that RHS of (5.13) reduces to $2/(z_j - 1)$, at leading order for large s. Hence, the system of saddle-point equations simplifies to a system of n_u identical, decoupled, equations. This is in fact one single equation determining the position of the n_u uncondensed roots. This equation can be called 'reduced saddle-point equation'. It turns out that the solutions of the reduced saddle-point equation, due to condensation itself, must obey certain property.

According to the standard picture, described in [47], the solutions of the saddle-point equations build up cuts in the large s limit, and these cuts move in the complex plane, as the parameters of the model (in our case x and y) are varied. Specifically, in our case, when $(x, y) \in \mathsf{D}$ (see figure 1), there is a cut, with complex conjugate end-points (let them be z_a and z_b), which lies to the left of the singularity at $z = 1$, and intersects the real axis on the segment $(0, 1)$. When we move (x, y) closer to the frozen region, $\mathsf{F}_{\rm NW}$, the end-points of the cut, while still complex conjugated, get closer to the real axis, with real part greater than 1. When (x, y) reaches the arctic curve, the end-points of the cut join at some value w on the real axis, $w > 1$, with the cut entangled around the singularity at $z = 1$. This corresponds to the total condensation of solutions of the saddle-point equations. When (x, y) enters the frozen region $\mathsf{F}_{\rm NW}$, the end-points separates, still sticking to the real axis, generating now a cut to the right of the singularity at $z = 1$.

Concentrating on the case of total condensation, the cut goes now from $z_a = w$ just above the real axis to the singularity at $z = 1$, surrounds it and comes back to $z_b = w$, running just below the real axis. The two portions of the cut which lie one in front of the other just above and below the real axis somehow compensate (the corresponding densities of roots cancel each other), and one is left with a pole at $z = 1$, describing the total condensation of roots. Hence, in this case, among the uncondensed roots, it is necessary to have a pair of coinciding roots, with value w, corresponding in fact to the end-points of the would-be cut, now collapsed to the pole at $z = 1$. Such pair of uncondensed root, can in principle lie anywhere on the portion of the real axis to the right of the condensation pole at $z = 1$. Their position, i.e. the value of $w \in [1, \infty)$, obviously depends on the position of point (x, y) on $\mathit{\Gamma}_{\rm NW}$. Thus the value of w naturally parameterizes the curve $\mathit{\Gamma}_{\rm NW}$ from the top contact point $(\kappa, 0)$ to the left one $(0, \kappa)$.

Summarizing, we arrive at the following alternative recipe for the derivation of the arctic curve: on the basis of the two properties of the multiple integral representation for EFP listed above, we assume that they are determined by the condition of condensation of roots. Then, given the system of saddle-point equations we impose condensation of 'almost all' its solutions, obtaining a reduced saddle-point equation, determining the position of the uncondensed roots. We then require the existence among them of two coinciding roots with value $w \in [1, \infty)$, which parameterizes the points on the arctic curve.

To illustrate and verify this recipe, we come back to saddle-point equation, (5.18), and implement the condensation of almost all roots. As already explained, the last term of LHS of (5.13) in the large s limit reduces to $2/(z_j - 1)$. As a result, this term combines with the first term and we end with the following reduced saddle-point equation

$$\frac{y}{z-1} - \frac{1-x}{z} + \frac{(1-y)t^2}{1+t^2 z} = 0. \tag{5.18}$$

This equation determines the position of those roots which survive in the complex plane and do not condense at $z = 1$.

We now require the existence among them of two coinciding roots. Noting that the numerator of (5.18) is of second order in z, we can simply require the vanishing of its discriminant, thus obtaining (5.16). Equivalently, denoting LHS of (5.18) by $F(z)$, we can require it to be of the form $F(z) = (z - w)^2 \widetilde{F}(z)$, with $\widetilde{F}(z)$ regular in the vicinity of w. This translates into a system of two equations $F(w) = 0$,

$F'(w) = 0$, linear in its unknowns x and y, with the solution

$$x = \frac{t^2 w^2}{t^2 w^2 + 1}, \qquad y = \frac{t^2(w^2 - 2w + 1)}{(t^2+1)(t^2 w^2 + 1)}, \qquad w \in [1, \infty). \tag{5.19}$$

It can be easily seen that, as w varies over the interval $[1, \infty)$, the point (x, y) above indeed describe the curve $\mathit{\Gamma}_{\mathrm{NW}}$, between the two contact points $(\kappa, 0)$ and $(0, \kappa)$. Elimination of parameter w from expressions (5.19) leads again to equation (5.16) for the arctic ellipse.

6. Arctic curves in the disordered regime

6.1. Condensation hypothesis. In the previous Section we have shown that the assumption of the correspondence between condensation of roots and the arctic curve allows one to derive this curve in a parametric form, through the requirement of a pair of coinciding roots for the reduced saddle-point equation. For the case considered there, the correspondence between condensation of roots and arctic curve can be verified by direct inspection of the form of the Green function, which indeed reduces to expression (5.15) for $(x, y) \in \mathit{\Gamma}_{\mathrm{NW}}$.

It turns out that in the general case, when the value of Δ is arbitrary, the method explained in Section 5.3 remains applicable! This observation is based on the fact that the two properties of the integrand of multiple integral representation for EFP listed in Section 5.3 appear to be totally independent of the value of Δ. This means that we can again assume that the arctic curve arises in correspondence to condensation of almost all roots of the saddle-point equations. It is to be emphasized, that in the general case however such correspondence cannot be verified, not even a posteriori (at least by the methods at our disposal), hence we call it here 'condensation hypothesis'.

Running a few steps forward, it worth to mention here that the only limitation which will restrict the final result to be valid only in the disordered regime ($|\Delta| < 1$) comes from formula (3.11) which will play an important role below in the analysis of the reduced saddle-point equation. For this reason we somehow restrict ourselves here to the disordered regime although the discussion is in fact rather general.

As just said, the 'condensation hypothesis' is strongly supported by the form of multiple integral representation (4.10) for EFP in the general case, satisfying the two crucial properties listed in Section 5.3. To show that the first property is indeed fulfilled, we have to consider, for $r, s = 1, \dots, N$, the integral

$$\begin{aligned} I_N^{(r,s)} = \frac{(-1)^{s(s+1)/2} Z_s}{s!(2\pi \mathrm{i})^s a^{s(s-1)} c^s} \oint_{C_1^-} \cdots \oint_{C_1^-} \prod_{j=1}^{s} \frac{[(t^2 - 2\Delta t) z_j + 1]^{s-1}}{z_j^r (z_j - 1)^s} \\ \times \prod_{\substack{j,k=1 \\ j \neq k}}^{s} \frac{1}{t^2 z_j z_k - 2\Delta t z_j + 1} \prod_{1 \leqslant j < k \leqslant s} (z_k - z_j)^2 \\ \times h_{N,s}(z_1, \dots, z_s) h_{s,s}(u_1, \dots, u_s) \, \mathrm{d}z_1 \cdots \mathrm{d}z_s. \end{aligned} \tag{6.1}$$

This integral differs from (4.10) only in the integration contour (recall that C_1^- denotes the closed negative-oriented contour in the complex plane, enclosing point $z = 1$, and no other singularity of the integrand). To show that quantity (6.1) is

identically equal to one, let us resort to another, essentially equivalent, representation

$$I_N^{(r,s)} := \frac{(-1)^s}{(2\pi\mathrm{i})^s} \oint_{C_1^-} \cdots \oint_{C_1^-} \prod_{j=1}^{s} \frac{[(t^2-2\Delta t)z_j+1]^{s-j}}{z_j^r (z_j-1)^{s-j+1}} \times \prod_{1\leqslant j<k\leqslant s} \frac{z_j-z_k}{t^2 z_j z_k - 2\Delta t z_j + 1}\, h_{N,s}(z_1,\dots,z_s)\,\mathrm{d}z_1\cdots\mathrm{d}z_s. \quad (6.2)$$

It is to be emphasized that equivalence of representations (6.1) and (6.2) simply follows from the fact that the integrand of (4.10) is the symmetrized version of the integrand of (4.8) (see [31] for details, and also Appendix C of [44] where a key identity has been proven). Performing integration in representation (6.2) in the variable z_s, and recalling property (4.6), the identity

$$I_N^{(r,s)} = 1, \qquad (r,s=1,\dots,N) \quad (6.3)$$

follows immediately by induction. In this way we observe that the first property, which states that the cumulative residue of the integrand for EFP over all variables $z_1,\dots,z_s$ at the pole $z=1$ is equal to 1, is indeed fulfilled for arbitrary value of Δ.

The second property, that the pole at $z=1$ for every integration variable $z_1,\dots,z_s$ is of order s, follows by simple inspection of representation (4.10). This means that we can again expect condensation of almost all roots of the saddle-point equations at $z=1$. Note that the other poles in the integrand of representation (4.10), being poles of small order even in the scaling limit, can only give subleading contributions, with respect to the stepwise behaviour generated by condensation at $z=1$. It is to be emphasized that although in the general situation we have no connection with the matrix model formulation any more, we can nevertheless represent the integrand in the exponential form with an 'action' which will contain, among many others terms, the term $s\sum_{j=1}^{s}\ln(z_j-1)$. Assuming validity of the condensation hypothesis we thus assume that this term still dominates when the parameters (x and y) are near the arctic curve and hence other terms have no relevance for the mechanism of condensation (although these other terms can contribute to the reduced saddle-point equation and therefore determine the arctic curve).

Thus we have just seen that the two main properties of the multiple integral representation (4.10) for EFP are fulfilled, strongly supporting the condensation hypothesis. Hence, we may apply the procedure explained in Section 5.3. This will be done in the remaining part of this section. Namely, we will derive the corresponding reduced saddle-point equation, and implement the condition of a pair of coinciding roots, to obtain the arctic curve in a parametric form.

6.2. 'Reduced' saddle-point equation. We thus assume condensation of solutions of saddle-point equations (4.12), and derive the corresponding reduced saddle-point equation. We start with setting n_c of the s variables z_k, $k=1,\dots,s$, to the value 1. We are left with a system of n_u equations in the n_u uncondensed variables, let them be z_j, $j=1,\dots,n_u$. In what follows, the fact that n_u/s vanishes in the scaling limit, see (5.17), plays a crucial role.

In saddle-point equation (4.12), let us consider the last term in the sum. As explained in Section 5.3, condensation of almost all roots reduces it to $2s/(z_j-1)$,

at leading order for large s. Similarly, for the remaining two terms in this sum, for large s, we have, respectively,

$$\sum_{\substack{k=1\\k\neq j}}^{s}\frac{t^2z_k-2\Delta t}{t^2z_jz_k-2\Delta t z_j+1}\longrightarrow s\frac{(t^2-2\Delta t)}{(t^2-2\Delta t)z_j+1}+o(s), \tag{6.4}$$

and

$$\sum_{\substack{k=1\\k\neq j}}^{s}\frac{t^2z_k}{t^2z_jz_k-2\Delta t z_k+1}\longrightarrow s\frac{t^2}{t^2z_j-2\Delta t+1}+o(s). \tag{6.5}$$

Further, due to property (4.6) function $h_{N,s}(z_1,\dots,z_s)$, appearing in the term after the sum in equation (4.12), simplifies to function $h_{N,n_u}(z_1,\dots,z_{n_u})$, which, in turn, for $N,s\to\infty$, and $n_u/N\sim 0$, can be evaluated for large s directly from its definition (4.5). In this way we obtain

$$\begin{aligned}\ln h_{N,s}(z_1,\dots,z_s)&\longrightarrow \ln h_{N,n_u}(z_1,\dots,z_{n_u})\\&=\sum_{j=1}^{n_u}\ln h_N(z_j)+o(s).\end{aligned} \tag{6.6}$$

Similarly, recalling that $u_k\to 0$ as $z_j\to 1$, see (4.11), and using property (4.7), we find that function $h_{s,s}(u_1,\dots,u_s)$, appearing in the last term of equation (4.12), simplifies, modulo an unessential factor, to function $h_{n_u,n_u}(u_1,\dots,u_{n_u})$. Recalling that $h_{n_u,n_u}(u_1,\dots,u_{n_u})$ is a polynomial of order n_u in each of its variables, we obtain that its logarithm for large s is estimated as $o(s)$. Thus we have

$$\begin{aligned}\ln h_{s,s}(u_1,\dots,u_s)&\longrightarrow \ln h_{n_u,n_u}(u_1,\dots,u_{n_u})+\sum_{j=n_u+1}^{s}\ln h_j(0)\\&=C_1s^2+C_2s+o(s).\end{aligned} \tag{6.7}$$

Here C_1 and C_2 are some quantities which do not depend on u_j $(j=1,\dots,n_u)$. After differentiating, we are left with a term estimated as $o(s)$, which is to be neglected, at the leading order in the large s limit.

As a result, we obtain that saddle-point equations (4.12) simplify to a set of n_u identical and decoupled equations,

$$F(z_j)=0,\qquad (j=1,\dots,n_u). \tag{6.8}$$

Here function $F(z)$ is given by

$$F(z):=\frac{y}{z-1}-\frac{1-x}{z}-\frac{yt^2}{t^2z-2\Delta t+1}+\left(\lim_{N\to\infty}\frac{\ln h_N(z)}{N}\right)', \tag{6.9}$$

where the scaling variables x and y are defined in (4.2).

To write the explicit form of the equation determining the location of uncondensed saddle-point solutions, we need to know the last term in the expression for $F(z)$. In what follows we shall need to consider the case of z real and positive. For these values we can use formula (3.11) for large N limit of function $h_N(z)$. From this formula, for the last term in (6.9) we obtain

$$\lim_{N\to\infty}\frac{\ln h_N(\gamma(\xi))}{N}=\ln\left(\frac{\sin\alpha(\lambda-\eta)\sin\alpha\xi\sin(\xi+\lambda-\eta)}{\alpha\sin(\lambda-\eta)\sin\xi\sin\alpha(\xi+\lambda-\eta)}\right). \tag{6.10}$$

Taking into account that function $\gamma(\xi)$, see (3.12), is a monotonously growing function, from $-\infty$ to $+\infty$, over the interval $\xi \in (-\lambda-\eta, \pi-\lambda-\eta)$, which is the interval of periodicity of $\gamma(\xi)$ (note that in fact $\gamma(\xi)$ is a rational function of $\cot\xi$), we can switch from function $F(z)$ to function $f(\xi)$, defined by

$$F(\gamma(\xi)) =: \frac{\sin(\lambda-\eta)\sin^2(\xi+\lambda+\eta)}{\sin(\lambda+\eta)\sin 2\eta}\, f(\xi). \tag{6.11}$$

Here the prefactor in fact is equal to $1/\gamma'(\xi)$. Direct calculation from (6.8) lead us to the following neat expression for this function

$$f(\xi) = x\,\varphi(\xi+\lambda) + y\,\varphi(\xi+\eta) - \Psi(\xi), \tag{6.12}$$

where function $\varphi(\xi)$ is given by (2.14) and function $\Psi(\xi)$ reads

$$\Psi(\xi) := \cot\xi - \cot(\xi+\lambda+\eta) - \alpha\cot(\alpha\xi) + \alpha\cot\alpha(\xi+\lambda-\eta). \tag{6.13}$$

Noting properties $\Psi(\pi-\lambda-\eta-\xi) = \Psi(\xi)$ and $\varphi(\pi-\xi) = \varphi(\xi)$, it easy to see that function $f(\xi)$ obeys the symmetry under the substitution $\xi \mapsto \pi-\lambda-\eta-\xi$ and simultaneous interchange of the coordinates, $x \leftrightarrow y$. This property of function $f(\xi)$ will lead to the diagonal-reflection symmetry of the arctic curve.

6.3. The arctic curve. To obtain the arctic curve from the reduced saddle-point equation, we will follow the recipe discussed in detail in Section 5.3. We thus have to require that function $F(z)$ has a double zero, which, moreover, must lie on the interval $[1,\infty)$. Denoting the value of this zero by w, we therefore require that $F(z) = (z-w)^2\tilde{F}(z)$, with $\tilde{F}(z)$ regular in the vicinity of w. This condition is equivalent to the system of two equations

$$F(w) = 0, \qquad F'(w) = 0. \tag{6.14}$$

These are equations for unknown x and y, which are functions of w. For each value of $w \in [1,\infty)$, values of x and y correspond to a point of the arctic curve, i.e., the solution of system (6.14) is just the arctic curve in a parametric form, with w being the parameter.

Taking into account the observation above that instead of function $F(z)$ we can use function $f(\xi)$, introduced by formula (6.11), we immediately obtain that system of equations (6.14) is equivalent to the following system of equations

$$f(\zeta) = 0, \qquad f'(\zeta) = 0, \tag{6.15}$$

where ζ is the new parameter which parameterizes the arctic curve, $w = \gamma(\zeta)$. The range of values of the original parameter w, varying in the interval $[1,\infty)$, corresponds $\zeta \in [0, \pi-\lambda-\eta]$.

We now solve the linear system of the two equations above, and arrive at the following result:

$$\begin{aligned} x &= \frac{\varphi'(\zeta+\eta)\Psi(\zeta) - \varphi(\zeta+\eta)\Psi'(\zeta)}{\varphi(\zeta+\lambda)\varphi'(\zeta+\eta) - \varphi(\zeta+\eta)\varphi'(\zeta+\lambda)}, \\ y &= \frac{\varphi(\zeta+\lambda)\Psi'(\zeta) - \varphi'(\zeta+\lambda)\Psi(\zeta)}{\varphi(\zeta+\lambda)\varphi'(\zeta+\eta) - \varphi(\zeta+\eta)\varphi'(\zeta+\lambda)}. \end{aligned} \tag{6.16}$$

These two equations constitute the parametric form of the top left portion, $\mathit{\Gamma}_{\mathrm{NW}}$, of the arctic curve, as the parameter ζ varies in the interval $[0, \pi-\lambda-\eta]$. The value $\zeta = 0$ corresponds to the contact point of the curve $\mathit{\Gamma}_{\mathrm{NW}}$ with the x-axis, and as

ζ increases, the whole curve $\Gamma_{\rm NW}$ is monotonously constructed, up to the contact point with the y-axis, at $\zeta = \pi - \lambda - \eta$.

Using the properties of the functions involved here, we can write the result in the form

$$x = X(\zeta), \qquad y = Y(\zeta), \qquad \zeta \in [0, \pi - \lambda - \eta], \tag{6.17}$$

where functions $X(\zeta) = X(\zeta; \lambda, \eta)$ and $Y(\zeta) = Y(\zeta; \lambda, \eta)$ are simply related by

$$X(\zeta) = Y(\pi - \lambda - \eta - \zeta). \tag{6.18}$$

Direct calculation gives

$$\begin{aligned} Y(\zeta) = {} & \frac{\sin^2\zeta \sin^2(\zeta+2\eta)\sin(\zeta+\lambda-\eta)\sin(\zeta+\lambda+\eta)}{\sin 2\eta \sin(\lambda-\eta)\big[\sin(\zeta+\lambda-\eta)\sin\zeta + \sin(\zeta+\lambda+\eta)\sin(\zeta+2\eta)\big]} \\ & \times \Bigg\{ \frac{\sin(\lambda-\eta)\sin(\lambda+\eta)}{\sin^2\zeta \sin(\zeta+\lambda+\eta)\sin(\zeta+\lambda-\eta)} \\ & \quad + \frac{\sin(2\zeta+2\lambda)}{\sin(\zeta+\lambda-\eta)\sin(\zeta+\lambda+\eta)} \, \frac{\alpha \sin\alpha(\lambda-\eta)}{\sin\alpha\zeta \sin\alpha(\zeta+\lambda-\eta)} \\ & \quad - \frac{\alpha^2 \sin\alpha(2\zeta+\lambda-\eta)\sin\alpha(\lambda-\eta)}{\sin^2\alpha\zeta \sin^2\alpha(\zeta+\lambda-\eta)} \Bigg\}. \end{aligned} \tag{6.19}$$

Formulae (6.17)–(6.19) represent the main result of the present paper.

As a comment to the result, it is worth to mention that in all examples discussed in the literature to date, the arctic curves (or frozen boundaries of limit shapes) always turn out to be algebraic curves. From the form of function $Y(\zeta)$ above it is straightforward to conclude that as far as the parameter $\alpha = \pi/(\pi - 2\eta)$ is irrational, the arctic curve of the domain-wall six-vertex model is a non-algebraic curve. This is the situation for generic weights of the six-vertex model in the disordered regime. On the other hand, the arctic curve is algebraic when α is a rational number, since then both $\cot\zeta$ and $\cot\alpha\zeta$, rationally entering in (6.19), can be expressed as rational functions of a suitably chosen parameter. In other words, the arctic curve in the domain-wall six-vertex model is rational only when the weights correspond to the so-called root-of-unity cases.

7. Particular cases and combinatorial applications

7.1. Alternating sign matrices. The arctic curve, whose general expression has been given in the previous Section, for arbitrary weights of the six-vertex model with domain wall boundary conditions in its disordered regime, is worth to be investigated in more detail when some of the parameters of the model are specialized to certain values. In this section we consider a few particular cases, some of which have a natural interpretation in the context of the limit shape of large alternating sign matrices. Indeed, our result for the arctic curve of the six-vertex model allows us to obtain the limit shapes of alternating sign matrices within q-enumeration schemes (for the disordered regime $0 < q \leqslant 4$, see below).

We recall that an alternating sign matrix is a matrix which has only 1's, 0's and -1's in its entries, obeying, moreover, the rule that in each row and each column of the matrix all nonzero entries alternate in sign, and the first and the last nonzero entries are 1's. In q-enumeration, denoted here as $A_N(q)$, each matrix has weight q^k where k is the number of -1's in its entries. For certain values of q, namely $q = 1, 2$, and 3, the numbers of q-enumerated alternating sign matrices, $A_N(q)$, are known

to be given by some factorized explicit expressions. These results, stated first as conjectures, remained challenging for their proofs for a long time, see [12, 32, 33] and references therein; the story and backgrounds of the problem can also be found in book [34].

A possible approach to alternating sign matrices exploits their close relationship with the domain-wall six-vertex model. Indeed, in [12] it was noticed that there is a one-to-one correspondence between N-by-N alternating sign matrices and configurations of the domain-wall six-vertex model on the N-by-N lattice. Due to this correspondence, $A_N(q)$ is equal, modulo a simple factor, to Z_N, the partition function of the domain-wall six-vertex model. The weights of this model have to satisfy the relations $a = b$ and, since c-weights comes in pairs, $c = a\sqrt{q}$. The first relation is fulfilled when $\lambda = \pi/2$ in (2.6), and the second one implies that q and Δ (recall that $\Delta = \cos 2\eta$) are related by

$$q = 2 - 2\Delta. \tag{7.1}$$

The precise relation between q-enumeration of N-by-N alternating sign matrices, $A_N(q)$, and the partition function Z_N (at $\lambda = \pi/2$) is

$$Z_N = a^{N^2} q^{N/2} A_N(q), \tag{7.2}$$

see, e.g., [12] for a discussion.

In the context of alternating sign matrices, the arctic curve of the domain-wall six-vertex model describes what is usually referred to as the 'limit shape'. Indeed, in their corner regions, alternating sign matrices mostly contain 0's, while in the interior they have many nonzero entries; as the size of matrices increases, the probability of finding 1's and -1's in the corner regions vanishes, while in the central region such probability remains finite [35]. As a result, in the scaling limit (i.e., when large matrices are scaled to a unit square) the arctic curve of the domain-wall six-vertex model precisely describes the shape of this central region (which is nothing but the region D, see Section 4).

A derivation of the limit shape of large q-enumerated alternating sign matrices at $q = 1$ and $q = 3$ (in addition to the well-known case of $q = 2$) was given in our previous paper [36]. There we used the observation of [41] that at $\eta = \pi/6, \pi/4, \pi/3$ (with $\lambda = \pi/2$), corresponding to the cases of $q = 1, 2, 3$, respectively, the Hänkel determinant standing in formula (2.13) for Z_N turns out to be related with certain classical orthogonal polynomials (this explains, additionally, the 'roundness' of $A_N(q)$ at $q = 1, 2, 3$). At these values of parameters the function $h_N(z)$ turns out to be expressible in terms of hypergeometric series and its large N asymptotic behaviour can be found directly, thus allowing us to derive the arctic curve on the basis of the 'condensation hypothesis'. Below we discuss several particular cases, and, in particular, how the results given in [36] follow from formulae (6.17)–(6.19), describing the arctic curve.

7.2. Particular cases. Let us consider the arctic curve for some particular values of weights of the disordered regime. As mentioned above, if the parameter λ is specialized to $\pi/2$, then the arctic curve also describes the limit shape of large alternating sign matrices, within the corresponding q-enumeration scheme. We consider here the cases which correspond to $q = 1, 2, 3$, and $q = 4$ where this last case is obtained as a limiting case, as $\Delta \to -1$. We also consider another limiting case, where q vanishes. Interestingly, in this case the limit shape tends to certain

nontrivial limiting curve, rather than becoming somehow degenerate or trivial; such limiting curve is discussed in more details below.

7.2.1. *The case* $\Delta = 0$. We start with the case $\Delta = 0$, or $\eta = \pi/4$. In this case, of course, we expect to reproduce the arctic ellipse discussed in detail in Section 5. Indeed, setting $\eta = \pi/4$ in formula (6.19), we obtain

$$Y(\zeta) = \frac{1}{2}(1 - \cos 2\zeta), \qquad \zeta \in \left[0, \tfrac{3\pi}{4} - \lambda\right]. \tag{7.3}$$

We also have $X(\zeta) = \frac{1}{2}(1 + \sin(2\zeta + 2\lambda))$, and we can easily eliminate parameter ζ in equations (6.17). As a result, we arrive again to equation (5.16), where $t := \tan(\lambda - \pi/4)$.

7.2.2. *The case* $\Delta = \frac{1}{2}$. The case $\Delta = 1/2$, or $\eta = \pi/6$, is interesting since at $\lambda = \pi/2$ the model is equivalent to the enumeration of alternating sign matrices (with $q = 1$). Specifying η to the value $\pi/6$ and setting $\lambda = \pi/2$, we find that expression (6.19) simplifies to

$$Y(\zeta) = 1 - \cos\zeta, \qquad \zeta \in \left[0, \tfrac{\pi}{3}\right]. \tag{7.4}$$

Correspondingly, we also have $X(\zeta) = 1 - \cos(\pi/3 - \zeta)$ and, eliminating parameter ζ, it can be found that the curve $\mathit{\Gamma}_{\mathrm{NW}}$ (the top-left portion of the arctic curve) is described by the equation

$$(2x-1)^2 + (2y-1)^2 - 4xy = 1\,, \qquad x, y \in \left[0, \tfrac{1}{2}\right]. \tag{7.5}$$

This curve describes the limit shape of large alternating signs matrices [36]. Interestingly, in comparison with the arctic circle, given by equation $(2y-1)^2+(2x-1)^2 = 1$, it has just single additional term $-4xy$ in LHS. The property of the curve $\mathit{\Gamma}_{\mathrm{NW}}$ to be given by a quadratic equation in the $\eta = \pi/6$ case holds only at $\lambda = \pi/2$. Indeed, just specifying $\eta = \pi/6$ but keeping λ generic, one finds from (6.19) that function $Y(\zeta)$ in this case is rather bulky; the curve $\mathit{\Gamma}_{\mathrm{NW}}$ turns out to be described by a tenth order equation.

7.2.3. *The case* $\Delta = -\frac{1}{2}$. The case of $\Delta = -1/2$, or $\eta = \pi/3$, will be treated here only at $\lambda = \pi/2$. At this choice of parameters the model is equivalent to q-enumeration of alternating sign matrices with $q = 3$, which is a well-known example of tractable enumeration (together with the cases $q = 1, 2$). Specifying in (6.19) $\eta = \pi/3$ and $\lambda = \pi/2$, we obtain

$$Y(\zeta) = 4\left[\frac{\sin(\frac{\pi}{3} - \zeta)\tan\zeta}{1 + 2\cos 2\zeta}\right]^2 \frac{11 + 12\cos 2\zeta - 2\cos 4\zeta}{6 - 3\cos 2\zeta - \sqrt{3}\sin 2\zeta}, \qquad \zeta \in \left[0, \tfrac{\pi}{6}\right]. \tag{7.6}$$

We also have $X(\zeta) = Y(\pi/6 - \zeta)$. For further analysis, it is convenient to rewrite the parametric formulae for the curve in terms of rational functions of a suitably chosen parameter. For example, choosing the parameter $w = \sin(\pi/6 + \zeta)/\sin(\pi/6 - \zeta)$, one obtains formulae for the curve given in [36]. Further, excluding the parameter w one can find the corresponding algebraic equation for the curve, which appears to be of the sixth order (see [36], equation (14)).

7.2.4. *The case* $\Delta = -1$. This case can be obtained as the limit from the disordered regime; in fact, the case of $\Delta = -1$ is often regarded as belonging to the disordered regime since the model is still disordered (at $\Delta = -1$ the model undergoes an infinite order phase transition). Denoting by v the rapidity variable of the model at $\Delta = -1$, the standard parameterization of the weights of this model reads

$$a = 1 + v, \qquad b = 1 - v, \qquad c = 2 \qquad (-1 < v < 1). \tag{7.7}$$

To fit this parametrization, one can perform the scaling in the parameters by taking the limit $\delta \to 0$, upon setting (see equation (2.6))

$$\lambda = \frac{\pi}{2} - v\delta, \qquad \eta = \frac{\pi}{2} - \delta. \tag{7.8}$$

Correspondingly, we also set $\zeta = p\delta$ and then equations (6.17) for the arctic curve will read $x = \widetilde{X}(p)$ and $y = \widetilde{Y}(p)$, where p is the new parameter which parameterizes the curve, $p \in [0, 1+v]$, and

$$\widetilde{X}(p) = \lim_{\delta\to 0} X(p\delta), \qquad \widetilde{Y}(p) = \lim_{\delta\to 0} Y(p\delta), \tag{7.9}$$

where δ also enters λ and η as given by (7.8). Functions $\widetilde{X}(p)$ and $\widetilde{Y}(p)$ also depend on v as a parameter and, due to (6.18), they satisfy $\widetilde{X}(p) = \widetilde{Y}(1+v-p)$. Explicitly, function $\widetilde{Y}(p)$ reads

$$\widetilde{Y}(p) = \frac{(2-p)^2}{4(1-v)\big[(1+v)(1-p)+p^2\big]}\Bigg\{1 - v^2 - \pi p^2(p-v)\,\frac{\cos\frac{\pi}{2}v}{\sin\frac{\pi}{2}p\,\cos\frac{\pi}{2}(p-v)} - \pi^2 p^2\big[1-(p-v)^2\big]\frac{\cos\frac{\pi}{2}v\;\cos\frac{\pi}{2}(2p-v)}{4\sin^2\frac{\pi}{2}p\,\cos^2\frac{\pi}{2}(p-v)}\Bigg\}, \tag{7.10}$$

where $p \in [0, 1+v]$. Clearly, in this case, contrarily to the three examples considered above, the arctic curve is not an algebraic one. In the case of $v = 0$, that is, when the weights satisfy $a = b$, the arctic curve describes the limit shape of large alternating sign matrices within the q-enumeration at $q = 4$.

7.2.5. *The case* $\Delta \to 1$. This case corresponds to $\eta \to 0$. For arbitrary λ and small η formula (6.19) reads

$$Y(\zeta) = \frac{1}{2\pi}(2\zeta - \sin 2\zeta) + O(\eta), \qquad \zeta \in [0, \pi - \lambda - \eta]. \tag{7.11}$$

Correspondingly, we also have $X(\zeta) = Y(\pi - \lambda - \eta)$. The subsequent analysis depends on whether or not, as η vanishes, the parameter λ is scaled accordingly.

Namely, the first possibility is to set $\lambda = \eta v$ or $\lambda = \pi - \eta v$ where v is a new rapidity variable ($v \geqslant 1$); this choice corresponds to approaching either of the two branches, $a > b$ or $a < b$, respectively, of the model at $\Delta = 1$. The weights of the model at $\Delta = 1$ are parameterized as $a = v \pm 1$, $b = v \mp 1$, and $c = 2$, where $v \geqslant 1$. The two choices of the signs corresponds to the two branches of the model at $\Delta = 1$. At $a > b$, we find, after eliminating the parameter ζ, that the curve $\mathit{\Gamma}_{\mathrm{NW}}$ is just the straight line: $x + y = 1$, where $x, y \in [0, 1]$. At $a < b$ the curve $\mathit{\Gamma}_{\mathrm{NW}}$ is just single point: $x = y = 0$. All this is in agreement with the fact that at $\Delta = 1$ the model is not disordered anymore; the region D, see figure 1, degenerates into the straight line $x + y = 1$ (if $a > b$) or $x = y$ (if $a < b$).

The second possibility, which appears to be also the most interesting, is to keep λ fixed as η vanishes. In the phase diagram of the six-vertex model in the a/c–b/c plane this corresponds to taking the limit into the deep infinity of the disordered region, rather than approaching either of the two branches of the $\Delta = 1$ model. In particular, setting $\lambda = \pi/2$ and neglecting small η corrections, one can easily find that the curve $\mathit{\Gamma}_{\mathrm{NW}}$ is given by the equation

$$x + y = \frac{1}{2} - \frac{1}{\pi}\cos\pi(x-y), \qquad x, y \in \big[0, \tfrac{1}{2}\big]. \tag{7.12}$$

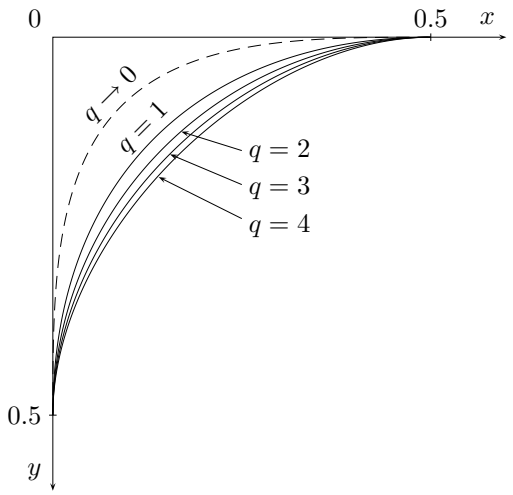


FIGURE 2. The limit shapes of the large alternating sign matrices within various q-enumeration schemes. As q vanishes, the limit shape tends to a limiting curve (dashed line), given by equation (7.12).

This equation has an interesting meaning in the context of alternating sign matrices: it is the limiting curve describing the limit shape as q tends to zero.

7.3. Discussion. A natural question concerns the qualitative behaviour of arctic curve (6.17)–(6.19) as one varies parameters of the model. In discussing some properties of the arctic curve it is useful to resort to numerical plotting. For example, considering the case of generic λ, we just mention here that as λ varies, the curve is deformed along one of the two diagonals according to the sign of $\lambda - \pi/2$. An example of the whole arctic curve $\mathcal{A}$ in a non-symmetric case is shown in figure 1. Namely, this figure shows the arctic curve at $\eta = \pi/6$ and $\lambda = 5\pi/12$.

Specializing to the case of $\lambda = \pi/2$ we can also discuss the arctic curve in application to the limit shape of large q-enumerated alternating sign matrices, with q and η related by (7.1). The relevance of formulae (6.17)–(6.19) in the context of alternating sign matrices is that they allow one to study the variation of the limit shape as q varies over the interval $(0, 4]$. In addition to the cases of $q = 1, 2, 3$ considered in [36], in figure 2 we plot also the limiting cases of $q = 4$ and $q \to 0$ (the latter shown by a dashed line). Note that, as expected, the disordered region (the area enclosed by the limit shape) is largest for $q \to 0$, and slowly decreases as q increases over the considered interval.

Comparing numerical plots of the arctic curve at various values of the parameters of the model we find that our results are completely compatible with all available numerical data [18, 19], which are however affected by large uncertainties, due to the huge technical difficulties in this kind of computer simulations. The most refined computer simulations available at the moment has been performed by Ben Wieland for the especially relevant case of alternating sign matrices at $q = 1$, corresponding to the value $\Delta = 1/2$. Pictures comparing these numerical data with the corresponding arctic curve, given by equation (7.5), are available [48].

Coming back to the qualitative behaviour of the arctic curve, we would like to focus again on the limiting curve, which, in the context of limit shapes of large alternating sign matrices, is referred above as the '$q \to 0$' curve. Note that such a curve exists for any fixed value of λ, as $\eta \to 0$ (see discussion in Section 7.2.5). Concerning the emergence of a non-trivial limiting curve, in hindsight, it is clear that this is ascribable to the fact that the two limits, $N \to \infty$, and $q \to 0$, do not commute.

8. Conclusions

In the present paper we have derived the arctic curve for the six-vertex model with domain wall boundary conditions, in its disordered regime. The derivation is essentially based on the exact expression in terms of a multiple integral for the emptiness formation probability, a correlation function which discriminates order and disorder. We have observed that in the scaling limit the arctic curve can be obtained as the condition that almost all solutions of the system of coupled saddle-point equations for the multiple integral representation of emptiness formation probability condense at the same, known, value. The explicit expression for the curve in parametric form shows that in general it is a non-algebraic curve; for special choices of weights of the model (the so-called root-of-unity cases) it simplifies to algebraic curves. We have also discussed combinatorial applications of the result to the problem of limit shapes of large alternating sign matrices within various enumeration schemes. In particular, we find that the limit shape of q-enumerated alternating sign matrices has a non-trivial limit as q tends to zero; furthermore, such limiting curve is described by a very simple equation.

Having established the expression of the arctic curve, a natural question concerns its fluctuations, which, in our approach, are related to the subleading corrections to the stepwise behaviour of emptiness formation probability in the scaling limit. In the case of domino tiling of Aztec diamond the fluctuations of the arctic circle are governed by the Tracy-Widom distribution and the Airy process [14, 15]. This results, which naturally extends to the case $\Delta = 0$ of the domain-wall six-vertex model [16], appears rather natural in view of the 'random matrix model' derivation of the arctic circle, provided in [37]. Indeed, the fluctuations of the arctic curve are expected to be governed by the fluctuations of the first eigenvalues evaporating from the logarithmic well where total condensation occurs, and these fluctuations are in turn known from the literature on Penner models (see, e.g., [47]) to be governed by the Tracy-Widom distribution. From the discussion of Sections 5 and 6, this pictures extends rather naturally to generic values of Δ in the disordered regime. On the basis of universality considerations, it is thus very tempting to argue that fluctuations of the arctic curve are still governed by the Airy process, at least in the disordered regime. A direct proof of this statement would be of great interest.

Another natural question concerns the extension of our results to the anti-ferroelectric regime, $\Delta < -1$. We recall that in this case (see Section 2.3) there are two different phase-separation curves, an outer one, which is the usual arctic curve, separating regions of ferroelectric order from an intermediate region of disorder, and an inner one, separating this region of disorder from a central region of anti-ferroelectric order. Since the emptiness formation probability detects spatial transition from order to disorder, the present approach can be used to address the

problem of the outer phase-separation curve. Most of its ingredients are independent of the value of Δ, and thus it can be directly applied to the anti-ferroelectric regime. In particular, in the special case of $\Delta \to -\infty$ (which is technically similar to the free-fermion case) the arctic curve can be readily derived, reproducing the result of paper [20]. For generic values of Δ in the anti-ferroelectric regime, the only open problem concerns the evaluation of the thermodynamic limit of function $h_N(z)$. Such evaluation would provide the solution to the problem of the outer phase-separation curve of the domain-wall six-vertex model for the whole anti-ferroelectric regime.

Acknowledgments

We thank Galileo Galilei Institute for Theoretical Physics for kind hospitality during the completion of this work. F.C. acknowledges partial support from MIUR, PRIN grant 2007JHLPEZ, and from the European Science Foundation program INSTANS. A.G.P. acknowledges partial support from INFN, Sezione di Firenze, from the Russian Foundation for Basic Research, grant 07-01-00358, and from the programme "Mathematical Methods in Nonlinear Dynamics" of Russian Academy of Sciences.

Appendix A. Partition function of partially inhomogeneous model and functions $h_{N,s}(z_1, \dots, z_s)$

Formula (2.12) is a special case of a more general determinant representation, known as Izergin-Korepin formula, which was originally derived for the model with inhomogeneous weights [25]. The weights are made position-dependent by attaching rapidity variables to each vertical and horizontal line, so that there are $2N$ rapidity variables in total instead of just one variable λ. Namely, the weights of the vertex lying at intersection of ith vertical and kth horizontal lines (we enumerate lines from right to left and from top to bottom) are parameterized as

$$a_{ik} = \sin(\lambda_i - \nu_k + \eta), \qquad b_{ik} = \sin(\lambda_i - \nu_k - \eta), \qquad c_{ik} = \sin 2\eta. \tag{A.1}$$

Correspondingly, the partition function is now a function of $2N$ rapidity variables $\lambda_1, \dots, \lambda_N, \nu_1, \dots, \nu_N$. In [25] the following representation was shown to be valid

$$Z_N(\lambda_1, \dots, \lambda_N; \nu_1, \dots, \nu_N) = \frac{\prod_{i,k=1}^{N} \sin(\lambda_i - \nu_k + \eta) \sin(\lambda_i - \nu_k - \eta)}{\prod_{1 \leqslant i < k \leqslant N} \sin(\lambda_i - \lambda_k) \sin(\nu_k - \nu_i)} \times \det M, \tag{A.2}$$

where M is an N-by-N matrix with the entries

$$M_{ik} := \varphi(\lambda_i - \nu_k) = \frac{\sin 2\eta}{\sin(\lambda_i - \nu_k + \eta) \sin(\lambda_i - \nu_k - \eta)}. \tag{A.3}$$

To obtain (2.12) from (A.2), one has to set $\nu_k = 0$ and $\lambda_i = \lambda$ $(i, k = 1, \dots, N)$. Due to the singularities in the denominator of representation (A.2), this has to be implemented as a limit, to be evaluated using l'Hôpital's rule.

In performing the limiting procedure to the homogeneous model there are some interesting intermediate situations. An important example is when the limit is performed only in one set of variables, say, $\nu_k \to 0$ $(k = 1, \dots, N)$ while all λ_i's are kept generic (and different from each other). Therefore, the weights are given by

$$a_i = \sin(\lambda_i + \eta), \qquad b_i = \sin(\lambda_i - \eta), \qquad c_i = \sin 2\eta. \tag{A.4}$$

and the partition function $Z_N(\lambda_1,\dots,\lambda_N) := Z_N(\lambda_1,\dots,\lambda_N;0,\dots,0)$ reads

$$Z_N(\lambda_1,\dots,\lambda_N) = \frac{\prod_{i=1}^N [\sin(\lambda_i+\eta)\sin(\lambda_i-\eta)]^N}{\left(\prod_{n=1}^{N-1} n!\right)\prod_{1\leqslant i<k\leqslant N}\sin(\lambda_k-\lambda_i)} \times \begin{vmatrix} \varphi(\lambda_1) & \dots & \varphi(\lambda_N) \\ \varphi'(\lambda_1) & \dots & \varphi'(\lambda_N) \\ \vdots & \ddots & \vdots \\ \varphi^{(N-1)}(\lambda_1) & \dots & \varphi^{(N-1)}(\lambda_N) \end{vmatrix}. \quad (A.5)$$

This case can be called partially inhomogeneous model: the model is homogeneous along one direction, but still inhomogeneous in the other one.

Having in mind this case as the starting point, one can consider, for any chosen s ($s=1,\dots,N$), the case where $\lambda_1,\dots,\lambda_s$ are different, but $\lambda_{s+1}=\dots=\lambda_N=\lambda$. One can still refer to such a situation as the partially inhomogeneous model. It turns out that in this case, the partition function is closely related to function $h_{N,s}(u_1,\dots,u_s)$ given by (4.5); in particular, the partition function (A.5) is related to function $h_{N,N}(u_1,\dots,u_N)$.

Let us define variables $\xi_1,\dots,\xi_N$ such that

$$\lambda_i = \lambda+\xi_i, \qquad i=1,\dots,N. \quad (A.6)$$

It is convenient to introduce the 'bare' partition function,

$$\widetilde{Z}_N(\xi_1,\xi_2,\dots,\xi_N) := \frac{Z_N(\lambda_1,\lambda_2,\dots,\lambda_N)}{Z_N(\lambda,\lambda,\dots,\lambda)}. \quad (A.7)$$

Below we shall treat ξ_i's as variables while λ is to be regarded as a parameter of the homogeneous model.

It is useful to consider first the case where all ξ_i's are zeros but one, say ξ_1, is kept nonzero. Denoting $\xi := \xi_1$ we straightforwardly have

$$\widetilde{Z}_N(\xi,0,\dots,0) = \frac{(N-1)!}{(\sin\xi)^{N-1}}\left[\frac{\varphi(\lambda)}{\varphi(\lambda+\xi)}\right]^N \frac{\widetilde{D}_N(\xi)}{D_N} \quad (A.8)$$

where, for later use, we have denoted

$$\widetilde{D}_N(\xi) := \begin{vmatrix} \varphi(\lambda) & \varphi'(\lambda) & \dots & \varphi^{(N-2)}(\lambda) & \varphi(\lambda+\xi) \\ \varphi'(\lambda) & \varphi''(\lambda) & \dots & \varphi^{(N-1)}(\lambda) & \varphi'(\lambda+\xi) \\ \vdots & \vdots & \ddots & \vdots & \vdots \\ \varphi^{(N-1)}(\lambda) & \varphi^{(N)}(\lambda) & \dots & \varphi^{(2N-3)}(\lambda) & \varphi^{(N-1)}(\lambda+\xi) \end{vmatrix}, \quad (A.9)$$

and D_N is given by (2.13). Note that in the case of one nonzero inhomogeneity one can always assume that it is attached to the last column (since $Z_N(\lambda_1,\dots,\lambda_N)$ is a symmetric function in its variables); thus we have chosen $\xi_2=\dots=\xi_N=0$ above.

To proceed further let us come back to the definition of the partition function as a sum over all configurations. The peculiarity of the domain wall boundary conditions is that they admit only one vertex of weight c in the last column; if this vertex is at rth position (counted from the top) then the first $(r-1)$ vertices are of weight b while the remaining $(N-r)$ vertices are of weight a. As it is has been explained in Section 3, the probability of having the c-weight vertex at rth position on last column is equal to $H_N^{(r)}$, the correlation function which is originally defined

as the probability of having the c-weight vertex at rth position on the first row, see (3.1). Due to this observation, the following relation is valid [33],

$$Z_N(\lambda_1,\lambda,\dots,\lambda)=Z_N\sum_{r=1}^{N}H_N^{(r)}\left[\frac{\sin(\lambda_1-\eta)}{\sin(\lambda-\eta)}\right]^{r-1}\left[\frac{\sin(\lambda_1+\eta)}{\sin(\lambda+\eta)}\right]^{N-r}, \tag{A.10}$$

where $Z_N=Z_N(\lambda,\dots,\lambda)$. Recalling that $h_N(z)=\sum_{r=1}^{N}H_N^{(r)}z^{r-1}$ and denoting

$$\gamma(\xi)=\frac{\sin(\lambda+\eta)}{\sin(\lambda-\eta)}\,\frac{\sin(\lambda+\xi-\eta)}{\sin(\lambda+\xi+\eta)} \tag{A.11}$$

we obtain that formula (A.10) actually reads

$$\widetilde{Z}_N(\xi,0,\dots,0)=\left[\frac{\sin(\lambda+\xi+\eta)}{\sin(\lambda+\eta)}\right]^{N-1}h_N(\gamma(\xi)). \tag{A.12}$$

More generally, as it has been first observed in [43] (at the special case $\lambda=\pi/2$) and proven in [31], for all $s=1,\dots,N$, one has

$$\widetilde{Z}_N(\xi_1,\dots,\xi_s,0,\dots,0)=\prod_{i=1}^{s}\left[\frac{\sin(\lambda+\xi_i+\eta)}{\sin(\lambda+\eta)}\right]^{N-1}h_{N,s}(u_1,\dots,u_s)\,, \tag{A.13}$$

where $h_{N,s}(u_1,\dots,u_s)$ is defined in (4.5), and

$$u_i:=\gamma(\xi_i). \tag{A.14}$$

The proof of (A.13) is based on formula (A.5) and some standard facts from the theory of orthogonal polynomials. We refer for further details and proofs to [31].

Finally we mention that formulae (A.8) and (A.12) provide a representation for generating function $h_N(z)$. This representation is used in Appendix B for a derivation of the large N leading term of $\ln h_N(z)$.

Appendix B. Large N limit for function $h_N(z)$

Our aim here is to show how formula (3.11) for the large N limit of function $h_N(z)$ can be derived. To this aim we extend here the method of [27], where the leading term of $\ln Z_N$ have been found. It is to be stressed that we assume that the weights correspond to the disordered regime only (see [28] for a discussion of why the same approach cannot be used for the anti-ferroelectric regime).

The approach is based on making use of some differential equations which can be obtained by means of the so-called Sylvester determinant identity. This identity relates the determinant of a matrix with a determinant of some other matrix whose entries are minors of the original matrix. Namely, let A be an n-by-n matrix, with entries $A_{j,k}$. Let us consider minors of degree p ($1\leqslant p\leqslant n$) of this matrix,

$$A\begin{pmatrix}i_1,i_2,\dots,i_p\\ k_1,k_2\dots,k_p\end{pmatrix}:=\begin{vmatrix}A_{i_1,k_1} & A_{i_1,k_2} & \dots & A_{i_1,k_p}\\ A_{i_2,k_1} & A_{i_2,k_2} & \dots & A_{i_2,k_p}\\ \vdots & \vdots & \ddots & \vdots\\ A_{i_p,k_1} & A_{i_p,k_2} & \dots & A_{i_p,k_p}\end{vmatrix}, \tag{B.1}$$

where $1\leqslant i_1<i_2<\dots<i_p\leqslant n$ and $1\leqslant k_1<k_2<\dots<k_p\leqslant n$. Let us introduce matrix B such that

$$B_{ik}:=A\begin{pmatrix}1,2,\dots,p,p+i\\ 1,2,\dots,p,p+k\end{pmatrix},\qquad i,k=1,\dots,n-p. \tag{B.2}$$

Hence, entries of B are minors of matrix A of degree $(p+1)$. The Sylvester identity reads

$$\det A = \left[A\begin{pmatrix}1,2,\dots,p\\1,2,\dots,p\end{pmatrix}\right]^{-(n-p-1)}\det B. \tag{B.3}$$

The standard proof of this identity is based on the Gauss algorithm, see, e.g., monograph [49] for further details. In all examples below we put $n = N+1$ and $p = N-1$, i.e., B will be a two-by-two matrix.

Let us consider first the partition function, Z_N, given by (2.12). We start with mentioning that for arbitrary N the partition function $Z_N = Z_N(\lambda)$ satisfies

$$Z_N(\lambda) = Z_N(\pi-\lambda), \qquad Z_N(\lambda)\big|_{\lambda=\eta} = (\sin 2\eta)^{N^2}. \tag{B.4}$$

Here, the first relation reflects the crossing symmetry of the model (since $b(\lambda) = a(\pi-\lambda)$), and the second one follows from the fact that if $b=0$ (or $a=0$) then there is exactly one configuration contributing to the partition function. As $N\to\infty$, one has [27]

$$Z_N = \exp\left(-N^2 f + O(N)\right), \tag{B.5}$$

where f is the free energy per site, the quantity of interest. To find f, let us consider the Hänkel determinant in (2.12), D_N, given by (2.13). As $N\to\infty$, we have

$$D_N = \left[\prod_{n=1}^{N-1}(n!)\right]^2 \exp\left(N^2\phi + O(N)\right), \tag{B.6}$$

where ϕ and f are related by

$$-f = \ln\sin(\lambda+\eta) + \ln\sin(\lambda-\eta) + \phi. \tag{B.7}$$

To compute ϕ, let us consider D_{N+1} and apply the Sylvester identity, with $n = N+1$ and $p = N-1$, which gives

$$D_{N+1} = \frac{1}{D_{N-1}}\begin{vmatrix}\partial_\lambda^2 D_N & \partial_\lambda D_N\\ \partial_\lambda D_N & D_N\end{vmatrix}. \tag{B.8}$$

In writing (B.8) we have taken into account that the first derivative of a Hänkel determinant changes the last row or the last column only, and the second derivative changes both the last row and the last column only. Relation (B.8) can be rewritten as

$$\frac{D_{N+1}D_{N-1}}{D_N^2} = \partial_\lambda^2 \ln D_N. \tag{B.9}$$

From (B.6) it follows that, as $N\to\infty$, the leading terms in each side of (B.9) are of order N^2; marching terms gives:

$$\mathrm{e}^{2\phi} = \partial_\lambda^2\phi. \tag{B.10}$$

To solve this equation it is convenient to define $W := \exp(-\phi)$, so that we arrive at

$$(\partial_\lambda W)^2 - W\partial_\lambda^2 W = 1. \tag{B.11}$$

Obviously, the general solution of this equation has the form

$$W = \frac{\sin(\alpha_1\lambda+\alpha_2)}{\alpha_1}, \tag{B.12}$$

where α_1 and α_2 are some constants. To fix these constants, let us turn to properties (B.4), and via relation (B.7) we obtain that they imply $W(\lambda) = W(\pi - \lambda)$ and $W(\lambda)\big|_{\lambda=\eta} = 0$, respectively. We find

$$\alpha_2 = \frac{\pi}{2}(1 - \alpha_1), \qquad \alpha_1 = \frac{\pi}{\pi - 2\eta}. \tag{B.13}$$

In terms of parameter α given by (2.17), we have $\alpha_1 = \alpha$ and $\alpha_2 = -\eta\alpha$, and therefore the result for ϕ reads

$$\phi = \ln\left(\frac{\alpha}{\sin\alpha(\lambda - \eta)}\right). \tag{B.14}$$

Substituting this result into (B.7), we readily reproduce formula (2.16) for the free energy in the disordered regime.

A detailed analysis of the large N expansion for the partition function of the domain-wall six-vertex model can be found in [39].

Let us now turn to the function $h_N(z)$. Due to formula (A.12), the large N limit of function $h_N(z)$ can be found from that of the partition function $\widetilde{Z}_N(\xi, 0, \dots, 0)$. This quantity is given by formula (A.8), where the nontrivial object is the last factor, the ratio of two determinants, which we denote

$$S_N(\xi) := \frac{\widetilde{D}_N(\xi)}{D_N} \tag{B.15}$$

(note that all quantities here also depend on λ, which is to be regarded now as a parameter). For any finite N we have the property (recall that $\widetilde{Z}_N(\xi, 0, \dots, 0)|_{\xi=0} = 1$)

$$S_N(\xi) \sim \frac{\xi^{N-1}}{(N-1)!}, \qquad \xi \to 0. \tag{B.16}$$

From the interpretation of $\widetilde{Z}_N(\xi, 0, \dots, 0)$ as the 'bare' partition function it follows that it can grow up at most exponentially as N increases, so that, as $N \to \infty$, we have

$$S_N(\xi) = \frac{1}{(N-1)!}\exp(N\psi(\xi) + o(N)). \tag{B.17}$$

We show now that $\psi(\xi)$ can be found as a solution of an ordinary first order differential equation (in the variable ξ). In turn, the result will imply formula (3.11).

Let us again use Sylvester identity, with $n = N + 1$ and $p = N - 1$, applying it to $\widetilde{D}_{N+1}$ and to $\partial_\lambda \widetilde{D}_{N+1}$ (see (A.9)), that gives

$$\begin{aligned} \widetilde{D}_{N+1}(\xi) &= \frac{1}{D_{N-1}}\begin{vmatrix} \partial_\lambda \widetilde{D}_N(\xi) & \partial_\lambda D_N \\ \widetilde{D}_N(\xi) & D_N \end{vmatrix}, \\ \partial_\lambda \widetilde{D}_{N+1}(\xi) &= \partial_\xi \widetilde{D}_{N+1}(\xi) + \frac{1}{D_{N-1}}\begin{vmatrix} \partial_\lambda \widetilde{D}_N(\xi) & \partial_\lambda^2 D_N \\ \widetilde{D}_N(\xi) & \partial_\lambda D_N \end{vmatrix}. \end{aligned} \tag{B.18}$$

In terms of function (B.15) these two relations read:

$$\begin{aligned}\frac{D_{N+1}D_{N-1}}{D_N^2}\,S_{N+1}(\xi) &= \partial_\lambda S_N(\xi)\\ \partial_\lambda S_{N+1}(\xi) + \frac{\partial_\lambda D_{N+1}}{D_{N+1}}\,S_{N+1}(\xi) &= \partial_\xi S_{N+1}(\xi) + \frac{D_N\partial_\lambda D_N}{D_{N+1}D_{N-1}}\,\partial_\lambda S_N(\xi),\\ &\quad + \frac{(\partial_\lambda D_N)^2 - D_N\partial_\lambda^2 D_N}{D_{N+1}D_{N-1}}\,S_N(\xi).\end{aligned} \tag{B.19}$$

The first relation here allows us to eliminate $\partial_\lambda S_N(\xi)$ and $\partial_\lambda S_{N+1}(\xi)$ in the second relation, and further, using (B.9) and shifting $N \mapsto N-1$, we obtain

$$\frac{D_{N+1}D_{N-1}}{D_N^2}\,S_{N+1}(\xi) + \left(\partial_\lambda \ln\frac{D_N}{D_{N-1}}\right) S_N(\xi) + S_{N-1}(\xi) = \partial_\xi S_N(\xi). \tag{B.20}$$

After dividing by $S_N(\xi)$, both sides of relation (B.20) are of order N in the large N limit; matching terms leads to the following ordinary first order differential equation:

$$\mathrm{e}^{2\phi}\,\mathrm{e}^{\psi(\xi)} + 2\partial_\lambda\phi + \mathrm{e}^{-\psi(\xi)} = \partial_\xi\psi(\xi). \tag{B.21}$$

Here the function ϕ is given by (B.14); explicitly, the equation reads

$$\frac{\alpha^2}{\sin^2\alpha(\lambda-\eta)}\,\mathrm{e}^{\psi(\xi)} - 2\alpha\cot\alpha(\lambda-\eta) + \mathrm{e}^{-\psi(\xi)} = \partial_\xi\psi(\xi). \tag{B.22}$$

Due to (B.16) we need the solution of this equation such that $\exp\psi(\xi) \sim \xi$ when $\xi \to 0$. The solution reads

$$\mathrm{e}^{\psi(\xi)} = \frac{\sin\alpha(\lambda-\eta)\sin\alpha\xi}{\alpha\sin\alpha(\xi+\lambda-\eta)}. \tag{B.23}$$

Recalling formulae (A.8), (B.15), and (B.17), we therefore find that, as $N \to \infty$,

$$\ln\widetilde{Z}_N(\xi,0,\ldots,0) = N\ln\left(\frac{\varphi(\lambda)}{\varphi(\lambda+\xi)}\,\frac{\sin\alpha(\lambda-\eta)\sin\alpha\xi}{\alpha\sin\alpha(\xi+\lambda-\eta)\sin\xi}\right) + o(N). \tag{B.24}$$

Finally, recalling that function $\varphi(\lambda)$ is given by (2.14) and that function $h_N(z)$ is related to $\widetilde{Z}_N(\xi,0,\ldots,0)$ by (A.12), we readily obtain expression (3.11), which is thus proven.

References

[1] W. Jockush, J. Propp, and P. Shor, *Random domino tilings and the arctic circle theorem*. E-print arXiv:math.CO/9801068.

[2] S. V. Kerov and A. M. Vershik, *Asymptotics of the Plancherel measure of the symmetric group and the limiting form of Young tableaux*, Sov. Math. Dokl. **18** (1977), 527–531.

[3] H. Cohn, M. Larsen, and J. Propp, *The shape of a typical boxed plane partition*, New York J. Math. **4** (1998), 137–165. E-print arXiv:math/9801059.

[4] M. E. Fisher, *Walks, walls, wetting and melting*, J. Stat. Phys. **34** (1984), 667–729.

[5] R. Cerf and R. Kenyon, *The low-temperature expansion of the Wulff crystal in the* 3*D Ising model*, Commun. Math. Phys. **222** (2001), 147–179.

[6] A. Okounkov and N. Reshetikhin, *Correlation function of Schur process with application to local geometry of a random* 3*-dimensional Young diagram*, J. Amer. Math. Soc. **16** (2003), 581–603. E-print arXiv:math/0107056 [math.CO].

[7] P. L. Ferrari and H. Spohn, *Step fluctuations for a faceted crystal*, J. Stat. Phys. **113** (2003), 1–46. E-print arXiv:cond-mat/0212456.

[8] R. Kenyon and A. Okounkov, *Limit shapes and the complex Burgers equation*, Acta Math. **199** (2007), 263–302. E-print arXiv:math-ph/0507007.

[9] R. Kenyon, A. Okounkov, and S. Sheffield, *Dimers and amoebae*, Ann. of Math. **163** (2006), 1019–1056. E-print arXiv:math-ph/0311005.
[10] B. Eynard, *A matrix model for plane partitions and (T)ASEP*. E-print arXiv:0905.0535.
[11] A. Borodin, V. Gorin, and E.M. Rains, *q-Distributions on boxed plane partitions*. E-print arXiv:0905.0679.
[12] N. Elkies, G. Kuperberg, M. Larsen, and J. Propp, *Alternating-sign matrices and domino tilings*, J. Algebraic Combin. **1** (1992), 111–132; 219–234.
[13] H. Cohn, N. Elkies, and J. Propp, *Local statistics for random domino tilings of the Aztec diamond*, Duke Math. J. **85** (1996), 117–166. E-print arXiv:arXiv:math/0008243 [math.CO].
[14] K. Johansson, *Non-intersecting paths, random tilings and random matrices*, Probab. Theory Related Fields **123** (2002), 225–280. E-print arXiv:math/0011250 [math.PR].
[15] K. Johansson, *The arctic circle boundary and the Airy process*, Ann. Probab. **33** (2005), 1–30. E-print arXiv:math/0306216 [math.PR].
[16] P. L. Ferrari and H. Spohn, *Domino tilings and the six-vertex model at its free fermion point*, J. Phys. A **39** (2006), 10297–10306. E-print arXiv:cond-mat/0605406.
[17] K. Eloranta, *Diamond ice*, J. Stat. Phys. **96** (1999), 1091–1109.
[18] O. F. Syljuåsen and M. B. Zvonarev, *Monte-Carlo simulations of vertex models*, Phys. Rev. E **70** (2004), 016118. E-print arXiv:cond-mat/0401491.
[19] D. Allison and N. Reshetikhin, *Numerical study of the* 6*-vertex model with domain wall boundary conditions*, Ann. Inst. Fourier (Grenoble) **55** (2005), 1847–1869. E-print arXiv:cond-mat/0502314.
[20] P. Zinn-Justin, *The influence of boundary conditions in the six-vertex model*. E-print arXiv:cond-mat/0205192.
[21] K. Palamarchuk and N. Reshetikhin, *The six-vertex model with fixed boundary conditions*, PoS (Solvay) (2008), 012.
[22] V. E. Korepin, *Calculations of norms of Bethe wave functions*, Commun. Math. Phys. **86** (1982), 391–418.
[23] L. A. Takhtadjan and L. D. Faddeev, *The quantum method of the inverse problem and the Heisenberg XYZ model*, Russian Math. Surveys **34** (1979), no. 5, 11–68.
[24] V. E. Korepin, N. M. Bogoliubov, and A. G. Izergin, *Quantum inverse scattering method and correlation functions*, Cambridge University Press, Cambridge, 1993.
[25] A. G. Izergin, *Partition function of the six-vertex model in the finite volume*, Sov. Phys. Dokl. **32** (1987), 878–879.
[26] A. G. Izergin, D. A. Coker, and V. E. Korepin, *Determinant formula for the six-vertex model*, J. Phys. A **25** (1992), 4315–4334.
[27] V. E. Korepin and P. Zinn-Justin, *Thermodynamic limit of the six-vertex model with domain wall boundary conditions*, J. Phys. A **33** (2000), 7053–7066. E-print arXiv:cond-mat/0004250.
[28] P. Zinn-Justin, *Six-vertex model with domain wall boundary conditions and one-matrix model*, Phys. Rev. E **62** (2000), 3411–3418. E-print arXiv:math-ph/0005008.
[29] N. M. Bogoliubov, A. G. Pronko, and M. B. Zvonarev, *Boundary correlation functions of the six-vertex model*, J. Phys. A **35** (2002), 5525–5541. E-print arXiv:math-ph/0203025.
[30] F. Colomo and A. G. Pronko, *On two-point boundary correlations in the six-vertex model with domain wall boundary conditions*, J. Stat. Mech. Theory Exp. (2005), P05010. E-print arXiv:math-ph/0503049.
[31] F. Colomo and A. G. Pronko, *Emptiness formation probability in the domain-wall six-vertex model*, Nucl. Phys. B **798 [FS]** (2008), 340–362. E-print arXiv:0712.1524 [math-ph].
[32] G. Kuperberg, *Another proof of the alternative-sign matrix conjecture*, Int. Math. Res. Not. **1996** (1996), 139–150. E-print arXiv:math/9712207.
[33] D. Zeilberger, *Proof of the refined alternating sign matrix conjecture*, New York J. Math. **2** (1996), 59–68. E-print arXiv:math/9606224.
[34] D. M. Bressoud, *Proofs and confirmations: The story of the alternating sign matrix conjecture*, Cambridge University Press, Cambridge, 1999.
[35] J. Propp, *The many faces of alternating-sign matrices*, Discr. Math. Theor. Comp. Sci. Proceedings **AA (DM-CCG)** (2001), 43–58. E-print arXiv:math/0208125.
[36] F. Colomo and A. G. Pronko, *The limit shape of large alternating-sign matrices*. E-print arXiv:0803.2697 [math-ph].
[37] F. Colomo and A. G. Pronko, *The Arctic Circle revisited*, Contemp. Math. **458** (2008), 361–376. E-print arXiv:0704.0362 [math-ph].

[38] R. J. Baxter, *Exactly solved models in statistical mechanics*, Academic Press, San Diego, CA, 1982.
[39] P. Bleher and V. Fokin, *Exact solution of the six-vertex model with domain wall boundary conditions. Disordered phase*, Commun. Math. Phys. **268** (2006), 223–284. E-print arXiv:math-ph/0510033.
[40] N. M. Bogoliubov, A. V. Kitaev, and M. B. Zvonarev, *Boundary polarization in the six-vertex model*, Phys. Rev. E **65** (2002), 026126. E-print arXiv:cond-mat/0107146.
[41] F. Colomo and A. G. Pronko, *Square ice, alternating sign matrices, and classical orthogonal polynomials*, J. Stat. Mech. Theory Exp. (2005), P01005. E-print arXiv:math-ph/0411076.
[42] F. Colomo and A. G. Pronko, *On the refined* 3*-enumeration of alternating sign matrices*, Adv. in Appl. Math. **34** (2005), 798–811. E-print arXiv:math-ph/0404045.
[43] F. Colomo and A. G. Pronko, *The role of orthogonal polynomials in the six-vertex model and its combinatorial applications*, J. Phys. A **39** (2006), 9015–9033. E-print arXiv:math-ph/0602033.
[44] N. Kitanine, J.-M. Maillet, N. A. Slavnov, and V. Terras, *Spin-spin correlation functions of the XXZ-*1/2 *Heisenberg chain in a magnetic field*, Nucl. Phys. B **641** (2002), 487–518. E-print arXiv:hep-th/0201045.
[45] R. C. Penner, *Perturbative series and the moduli space of Riemann surfaces*, J. Diff. Geom. **28** (1988), 35–53.
[46] L. Paniak and N. Weiss, *Kazakov-Migdal model with logarithmic potential and the double Penner matrix model*, J. Math. Phys. **36** (1995), 2512–2530. E-print arXiv:hep-th/9501037.
[47] J. Ambjorn, Yu. Makeenko, and C. F. Kristjansen, *Generalized Penner models to all genera*, Phys. Rev. D **50** (1994), 5193–5203. E-print arXiv:hep-th/9403024.
[48] B. Wieland. Message of Jan 10, 2008 on Domino Forum; pictures are available at WWW page http://math.brown.edu/~wieland/asm-frozen/.
[49] F. R. Gantmacher, *The theory of matrices*, Translated from the Russian by K.A. Hirsch, Vol. 1, Chelsea Publishing, New York, 1959.

INFN, Sezione di Firenze, Via G. Sansone 1, 50019 Sesto Fiorentino (FI), Italy
E-mail address: colomo@fi.infn.it

Saint Petersburg Department of V.A. Steklov Mathematical Institute of Russian Academy of Sciences, Fontanka 27, 191023 Saint Petersburg, Russia
E-mail address: agp@pdmi.ras.ru